ni

NATIONAL AERONAUTICS AND SPACE ADMINISTRATION

Technical Report 32-1180

Determination of Footpad Penetration Depth from Surveyor Spacecraft Shadows

R. L. Spencer

JET PROPULSION LABORATORY
CALIFORNIA INSTITUTE OF TECHNOLOGY
PASADENA, CALIFORNIA

October 15, 1967

NATIONAL AERONAUTICS AND SPACE ADMINISTRATION

Technical Report 32-1180

Determination of Footpad Penetration Depth from Surveyor Spacecraft Shadows

R. L. Spencer

Approved by:

L. D. Jaffe
Surveyor Project Scientist

H. H. Haglund, *Manager*
Surveyor Project

JET PROPULSION LABORATORY
CALIFORNIA INSTITUTE OF TECHNOLOGY
PASADENA, CALIFORNIA

October 15, 1967

Contents

Tables

Figures

Contents (contd)

Figures (contd)

Abstract

A simple form of optical triangulation, using the *Surveyor* TV camera view angles and sun shadows, is used to determine the elevation of the lunar surface relative to the *Surveyor* spacecraft. A group of these elevation points, near the spacecraft footpads 2 and 3, were calculated to indicate the footpad penetration depths. The limitations and potential applications of the method of analysis are discussed. A computer program designed to handle the shadow analysis calculations on the IBM 1620 computer is presented in Appendixes A, B, and C.

Determination of Footpad Penetration Depth from *Surveyor* Spacecraft Shadows

I. Introduction

More than 11,000 TV pictures were obtained during *Surveyor* Mission A. These TV pictures were taken by one fixed-position survey camera. Despite this voluminous collection of images, answers to many questions about the spacecraft penetration depth and the lunar surface elevation and range remain doubtful. This report presents an attempt to extract more definitive answers from these pictures.

The method of solution is a form of optical triangulation based on a knowledge of (1) the geometric relationship between the TV camera and other fixed elements of the *Surveyor* spacecraft, (2) elevation and direction of the sun as a function of time at the landing site, and (3) TV photographic images of spacecraft components and their shadows on the lunar surface.

Many of the *Surveyor* TV frames display useful shadow images. If knowledge of the other factors is correct, the shadowed surface could be located in three-dimensional space. A series of pictures of several components taken over an extended time period would give a family of data points that could be combined to form a simple elevation map of the lunar surface around the spacecraft. The penetration depth of the *Surveyor* footpads could be estimated from this profile map.

The methodology for getting three-dimensional data from individual, two-dimensional TV pictures, known as the *Surveyor* Shadow Analysis, has progressed through three main stages. First, the general mathematical relationships needed to solve the problem were selected and test problems were tried. The solution uses analytical geometry and trigonometry. The general approach is simple; however, since directional vectors are involved, signs and directions must be checked carefully and kept consistent throughout the calculations.

Next, the solution method for the analysis of several typical TV pictures was applied. The *Surveyor* Mission A picture data file was scanned and 22 frames were selected. An electronic desk calculator was used for all numerical calculations. Results of this analysis are presented in later sections of this report.

This error analysis proved more complex than the original problem solution and much too time consuming for manual calculation. Therefore, the third step involved preparation of a computer program to handle the basic solution and also run the error analysis.

II. Shadow Analysis Procedure

The basic technique used for the shadow analysis can be more clearly understood by referring to the first two illustrations. Figure 1 is a wide-angle photograph taken on Day 157 of Mission A. This frame shows the auxiliary battery box and its shadow on the surface of the moon. The rows and columns of small, reference reseau marks distributed over the frame should also be noted. The GMT time of transmission, as recorded in the TV data file, is also of importance.

The photographic data reduction provides the view angle, V, as seen from the TV position, between the image of the spacecraft object and its shadow on the lunar surface. This is determined by measuring the linear spacing between the object and its shadow in the photograph and converting this length into angular units by reference to the reseau marks. The angle between adjacent reseau marks is a calibrated function of the focal length of the TV camera lens

$$\text{Angle } V = \frac{(RF)\,(SW)}{R} \tag{1}$$

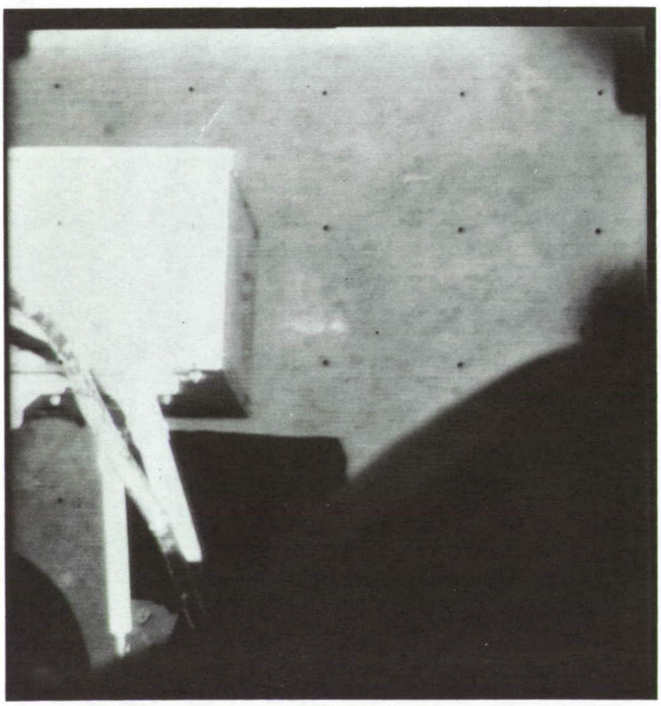

Fig. 1. *Surveyor I* TV photograph showing the auxiliary battery and its shadow on the lunar surface (Day: 157, Time: 13:59:34)

where

RF = reseau reference angle

SW = length of shadow view line

R = reseau mark spacing

The sun elevation angle and azimuth direction, in selenographic coordinates, must be determined for the GMT time of the TV frame. When the orientation of the spacecraft on the lunar surface has been defined, the sun angles can be related to the picture data by converting all angles into a common reference coordinate system.

The space geometry for the shadow analysis could have been related to any of several coordinate systems, including selenographic, TV camera centered or spacecraft centered. A modified spacecraft coordinate system was chosen to simplify the calculations. In this system, the vertical Z axis is equivalent to the normal spacecraft system. The XY plane, or the O level for the Z axis, has been positioned at the level of the lowest rigid spaceframe members. This plane also bisects the landing leg hinge centerlines. Positions above this plane have a positive value for Z. The X axis, the XZ plane, and the YZ plane are the same as in the normal spacecraft system. However, the Y axis was reversed from the usual spacecraft orientation to simplify a problem in the computer program. Any position on the spacecraft or on the surface around it can be located by its unique XYZ coordinate values. Directional vector lines can be identified by their respective α, β, and γ direction cosine angles made with the X, Y, and Z axes.

The geometric relationships between the TV camera and the shadow object are illustrated in Fig. 2. In the figure, the *Surveyor* spacecraft is shown in the post-landed position. The auxiliary battery box is the spacecraft component used in this example, and its shadow can be seen on the ground below. If straight lines were drawn between the TV camera (V), the outboard corner of the battery box (N), and its shadow on the surface (D), they would form a plane triangle that could be solved to locate the surface position at D.

The location of the TV camera elevation mirror reference point $(X_1Y_1Z_1)$ and the position of the battery box corner $(X_2Y_2Z_2)$ can be established in the modified spacecraft coordinate system. Assume that the view angle V, and the sun's direction angles have been determined from TV picture data. The straight line between the TV camera mirror $(X_1Y_1Z_1)$ and the spacecraft component considered $(X_2Y_2Z_2)$ is identified as L and its length and

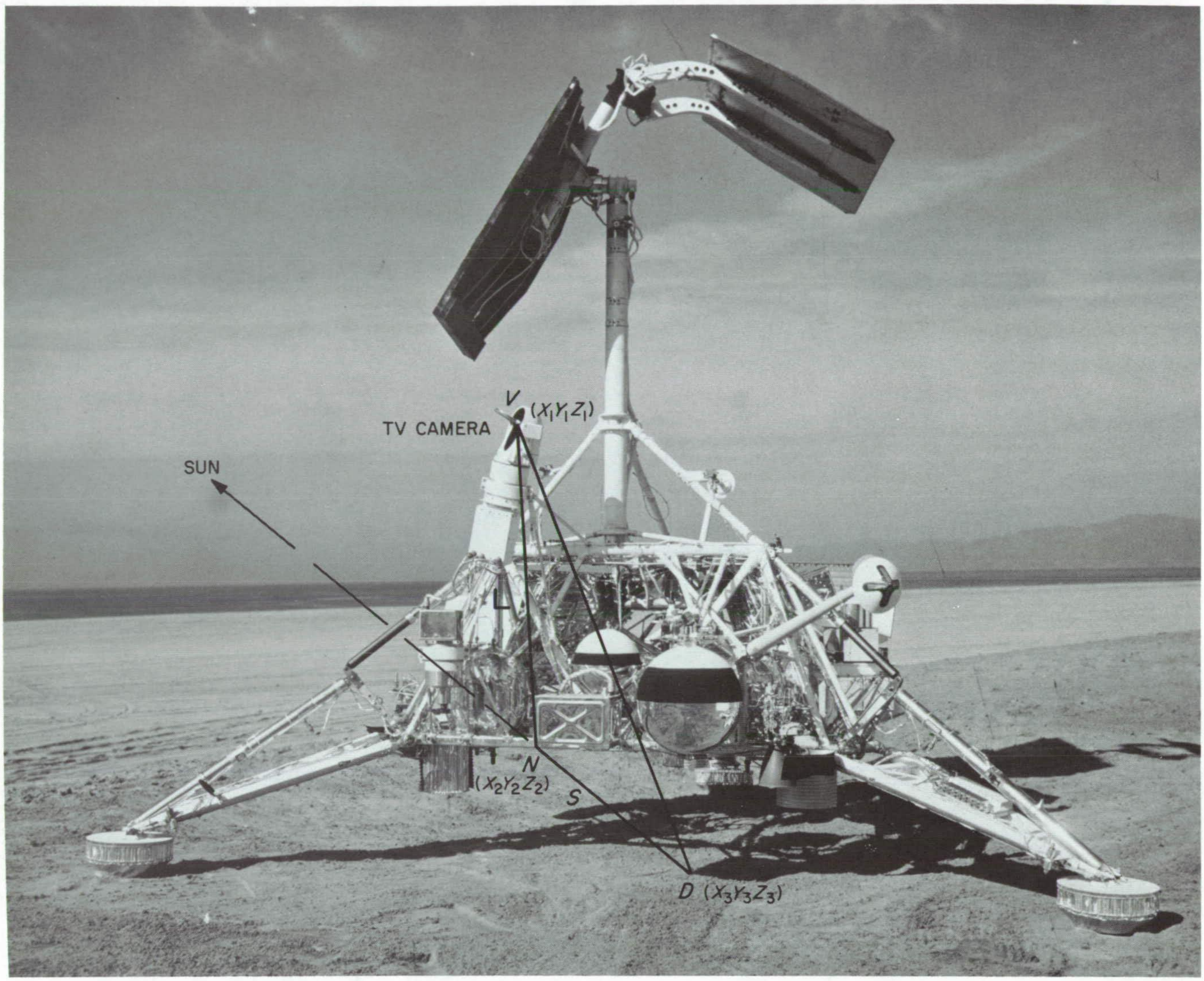

Fig. 2. *Surveyor I* spacecraft with shadow analysis triangle

direction cosine angles are obtained from the following equations:

$$\text{length } L = [(X_2 - X_1)^2 + (Y_2 - Y_1)^2 + (Z_2 - Z_1)^2]^{1/2} \quad (2)$$

$$\cos \alpha = \frac{X_2 - X_1}{L} \quad \text{(angle with } X \text{ axis)} \quad (3)$$

$$\cos \beta = \frac{Y_2 - Y_1}{L} \quad \text{(angle with } Y \text{ axis)} \quad (4)$$

$$\cos \gamma = \frac{Z_2 - Z_1}{L} \quad \text{(angle with } Z \text{ axis)} \quad (5)$$

For a better understanding of the next step in the shadow solution, the geometry of the TV camera optical system must be considered. The front nodal point of the camera lens, represented by the apex of the viewing angle V, is located in the camera housing, several inches below the elevation mirror. Its exact location depends on the focal length and focus settings of the camera lens. The distance between the elevation mirror and the front nodal point can range from 11.4 in. for a narrow-angle (100 mm), 4-ft focus setting, to approximately 6.4 in. for a wide-angle (25 mm), infinity focus combination (Fig. 3).

The image of the front nodal point $(X_pY_pZ_p)$ is located an equivalent distance (L_p) behind the elevation mirror and changes position each time the mirror is moved in

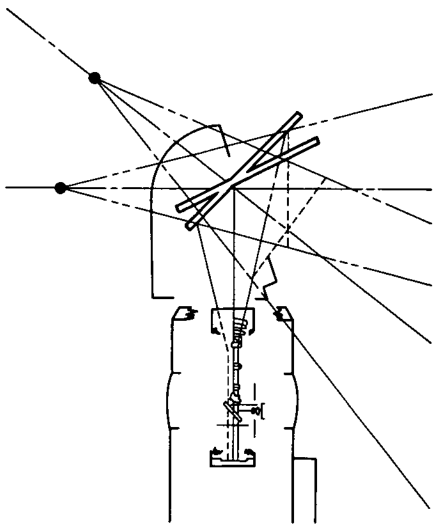

Fig. 3. Optical geometry of the survey TV camera

azimuth or elevation. The total distance from the nodal point $(X_pY_pZ_p)$ to the object point $(X_2Y_2Z_2)$ is the combined sum of L and L_p.

The value of L_p is an independent input for each individual solution, and its value can be determined from a table of focus-focal length factors. However, for purposes of discussion, L_p is assumed to be 6.5 in. for all wide-angle frames and 11 in. for narrow-angle frames.

If it is assumed that the camera optical axis passes through the elevation mirror pivot axis, then the line segments L_p and L will be parallel and will meet at $X_1Y_1Z_1$. The location of $X_pY_pZ_p$ can then be determined by the equations

$$X_p = (\cos\alpha)(L + L_p) - X_2 \qquad (6)$$

$$Y_p = (\cos\beta)(L + L_p) - Y_2 \qquad (7)$$

$$Z_p = (\cos\gamma)(L + L_p) - Z_2 \qquad (8)$$

The sun's direction angles are often given in the spherical coordinates of the elevation above the horizon (θ) and the azimuth from the spacecraft X axis (ϕ). These angles can be converted into polar form by the relations

$$\cos\alpha' = \cos\theta\cos\phi \qquad \text{(sun angle with } X \text{ axis)} \qquad (9)$$

$$\cos\beta' = \cos\theta\sin\phi \qquad \text{(sun angle with } Y \text{ axis)} \qquad (10)$$

$$\cos\gamma' = \sin\theta \qquad \text{(sun angle with } Z \text{ axis)} \qquad (11)$$

It should be noted that the prime symbol is used for the sun angles. The length of line ND is still unknown, but its direction in space must be the same as the sun vector line with angles α', β', and γ'. With the direction cosine angles for the two intersecting lines, VN and ND, their intersect angle (N) can be calculated as follows:

$$\cos N = \cos\alpha\cos\alpha' + \cos\beta\cos\beta' + \cos\gamma\cos\gamma' \qquad (12)$$

With angle V, this gives two angles and one side of a plane triangle

$$\text{angle } D = \pi - (N + V) \qquad (13)$$

Other parts of the triangle can be solved by the law of sines

$$\left.\begin{aligned} \frac{S}{\sin V} &= \frac{(L + L_p)}{\sin D} \\ S &= \frac{(L + L_p)\sin V}{\sin D} \end{aligned}\right\} \qquad (14)$$

Side S is the length of the shadow line in three-dimensional space. The coordinates for the shadow point $(X_3Y_3Z_3)$ can now be calculated by using a variation of the direction cosine formulas

$$\cos\alpha' = \frac{X_2 - X_3}{S} \qquad X_3 = X_2 - S\cos\alpha' \qquad (15)$$

$$\cos\beta' = \frac{Y_2 - Y_3}{S} \qquad Y_3 = Y_2 - S\cos\beta' \qquad (16)$$

$$\cos\gamma' = \frac{Z_2 - Z_3}{S} \qquad Z_3 = Z_2 - S\cos\gamma' \qquad (17)$$

All of the calculated solutions for Z_3 have a negative value, since the ground level is several inches below the reference XY plane. Conversion of Z_3 values into relative footpad penetration depths can be done by subtracting the normal elevation value for the bottom of the footpads.

This step completes the general procedure for the shadow analysis. It can be used with selected *Surveyor* TV pictures from Mission A or from subsequent *Surveyor* missions. The images of a known spacecraft component and its shadow on the lunar surface should be contained within the same TV frame to minimize the errors in the angle V. When the images are in adjacent frames, careful mosaic work can combine the two photographs for analysis. This limits the analysis of the surface to the area under or near the spacecraft on which shadows fall.

However, this is the area about which information was needed to determine the footpad penetration depth.

The TV azimuth and elevation angles were not used as data inputs. These angles were avoided for two reasons. The tilted camera axis would greatly complicate the calculations and require conversion into and out of the spacecraft coordinate system. The TV identification data, as recorded during Mission A, contained occasional dropouts and gross errors and some unexplained angular shifts that would cause large errors in the calculated results. Should these problems be eliminated by improved mission operations or post-mission data reduction, then the shadow analysis could be extended to more distant areas where shadows will be cast when the sun is at lower angles. In such cases, the TV camera pointing coordinates would locate the shadow and establish an angle V even when the object, such as the solar panel, is not directly visible to the camera. This would be the next logical stage of development for the shadow analysis. A discussion of this phase of analysis will not be undertaken herein.

III. Data Assumptions

The general approach for the shadow analysis is simple. The accuracy of the results depends on the care exercised in the selection and interpretation of the data sources. When numerical data from several sources must be evaluated and selected, it is inevitable that many assumptions that will influence the results will be made. Before discussing the results of calculations, based on data from Mission A, the assumptions that preceded them should be examined. The general solution equations were kept free of limiting factors that only apply to Mission A.

The first assumption concerns the orientation of the spacecraft on the lunar surface. For Mission A, the orientation angles adopted were those reported in the Hughes Aircraft Company memorandum on sun/earth positions (Ref. 1). Conclusions reached by Hughes Aircraft Company personnel were based on data inputs from the spacecraft gyros, the antenna and solar panel positions, and the TV camera star sightings. The slightly different angles recorded in the JPL Mission Report (Ref. 2) were apparently based only on the star sightings. The differences are small, but the deciding factor was that the Hughes Aircraft Company memorandum contained a complete list of sun and earth direction angles, calculated in spacecraft coordinates, which could be used with a minimum of additional conversion.

The variable focal-length TV lens is normally used at the wide-angle (25 mm) and the narrow-angle (100 mm) settings. It was assumed that the operation of the lens was normal and that all pictures were taken at one of these two positions. At these focal lengths, the angular spacing between the rows and columns of reseau marks (parameter RF in Eq. 1) is assumed to be 5 deg at WA and 1.25 deg at NA. These values would be limited to the footpad focus distances. The reseau angle varies with focus changes and would be approximately 10% larger at infinity focus. The effects of optical or geometric distortions in the camera lens were neglected. On later *Surveyor* missions, a test record of geometric distortion will be included as part of the camera calibration; this information, however, was not available for Mission A. The reference point for the TV camera was assumed to be the center of the elevation mirror hinge line. The coordinate values for this point were used as X_1, Y_1, and Z_1 in the equations.

The location of the TV camera ($X_1Y_1Z_1$) and of other spacecraft components ($X_2Y_2Z_2$), referenced to the modified spacecraft coordinate system, should ideally be based on measurements of the actual flight hardware or on the best documentation record of this hardware. However, such direct contact with assembled flight spacecraft is discouraged for obvious reasons. The other space frames and test vehicles available at the time of the search contained structural differences that would have been misleading. The assembly drawing recommended as the best source for the needed information was the *Surveyor* Spacecraft A-21 Configuration Drawing (Ref. 3). Scaling measurements from a print are usually discouraged for many reasons including that of paper shrinkage. However, this drawing contains a built-in linear scale that can be used to correct for some of the paper shrinkage. Therefore, for the purpose of the calculations on the Mission A data, the spacecraft location measurements were taken from a J-size print of the referenced drawing. The reduced microfilm copies contained noticeable distortion and would not be usable for this purpose.

The results could also be influenced by the final deflection angle of the landing legs after the spacecraft comes to rest. The legs normally are at an angle of 18 deg, as measured from a level surface. Leg angle pots provide a telemetry voltage that is transmitted after landing and that is calibrated during spacecraft checkout. However, the information from this source is not without its limitations. The pot voltage is not set for zero, but just measured when the legs are hanging free with no contact with the ground. The telemetry data have an error band equivalent to ±1 deg. The telemetry data from Mission A could be interpreted as being somewhere between 16 and 18 deg, depending on the choice of tolerances.

Therefore, for purpose of these calculations, it was assumed that all three legs are resting at the normal angle of 18 deg. Different angles will affect the Z_2 values for the footpad and other components mounted on the lower portions of the leg. The errors in Z_3 would be mainly from the direct contribution of Z_2 in Eq. (17).

The top of footpad 2 is tilted, toe down and heel up, at an angle of approximately 6 deg referenced to the XY plane. This was determined experimentally by comparing shadow angles of pictures taken late in the lunar day. This assumed tilt angle affects the Z_2 value for portions of the footpad top.

IV. Data Calculations and Results

Twenty-two TV pictures were selected from the Mission A data. These pictures were chosen to help define the area around footpads 2 and 3. Some of these pictures contained two or more possible shadow data points so that 30 solutions were calculated. The shadows were cast by eight different spacecraft components. The numerical values assigned to each $X_2Y_2Z_2$ position, and the parameters calculated at several steps of the solutions, are tabulated in Tables 1, 2, and 3. The modified spacecraft coordinate system and the definition for angular measurements are illustrated in Fig. 4. This figure also indicates the surface area included in the several solutions.

The interpretation of the view angle V has a potential source of error that should be pointed out. This error concerns the reseau spacing width, parameter R, in

Table 1. Spacecraft I.D. parameters used in the shadow solutions[a]

Spacecraft item	S/C positions			Distance and direction from TV camera			
	X_2, in.	Y_2, in.	Z_2, in.	L, in.	Cos α	Cos β	Cos γ
TV camera reference ($X_1Y_1Z_1$)	13.0	27.4	44.0	—	—	—	—
Footpad 2 gas jet	60.5	39.6	−9.0	72.20	0.6578	0.1689	−0.7340
Footpad 3 gas jet	−60.5	39.6	−9.0	91.43	−0.8041	0.1334	−0.5798
Leg 2 lock fixture	58.5	34.0	−4.1	66.53	0.6842	0.0992	−0.7233
Leg 3 lock fixture	−58.5	34.0	−4.1	86.42	−0.8272	0.0764	−0.5565
Leg 2 TV target (top)	57.0	36.3	−5.3	66.67	0.6606	0.1336	−0.7402
Footpad 2, top-center	66.3	38.4	−13.6	79.2	0.6729	0.1388	−0.7272
Footpad 2, top (position 10)	67.8	44.3	−13.9	81.49	0.6724	0.2074	−0.7105
Footpad 2, top (position 3)	69.2	33.0	−13.6	80.66	0.6972	0.0694	−0.7146
Footpad 3, top-center	−66.3	38.4	−13.6	98.6	−0.8042	0.1115	−0.5841
Footpad 3, top (position 3)	−65.0	43.8	−13.6	98.33	−0.7932	0.1667	−0.5857

[a] Positions on top of footpad are referenced as per clock positions.

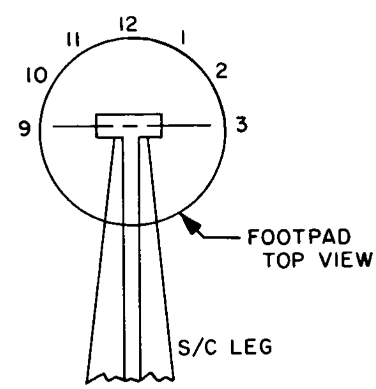

Eq. (1). For purposes of this report, the separations between the etched reseau marks on the face of the TV camera tube can be considered equal. The separations observed in a typical *Surveyor I* photograph are noticeably unequal, with the difference approaching 10% in some frames. This distortion is a combination of all the nonlinear deflection and scan problems in the camera and the ground recording equipment. As a result, no one value for R can be used for all sections of a *Surveyor* photograph. To reduce errors in the angle V, the reseau marks measured are those that are over or adjacent to the portion of the picture area containing the shadow image. For the 22 pictures considered in this study, enlarged 8 × 10-in. glossy prints and a pair of drafting dividers were used to make the data measurements. When a diagonal shadow ran between reseau marks with widely different row and column spacing, the calculated reseau diagonal spacing distance was used for parameter R. Careful attention at this stage of data reduction will keep the errors in R below 1%.

Table 2. *Surveyor* shadow study data on photographs near footpads 2 and 3

I.D.	Day	GMT	Sun angles		Sun direction cosines			Solution
			El θ, deg	Az ϕ, deg	Cos α'	Cos β'	Cos γ'	
				Area east of footpad 3				
22124	161	09:43:05	51.7	264.7	−0.0573	−0.6171	0.7848	1
22125	161	09:43:11	51.7	264.7	−0.0573	−0.6171	0.7848	2
27627	161	14:42:53	49.13	265.05	−0.0565	−0.6519	0.7562	3
17264	161	15:01:18	49.0	265.1	−0.0560	−0.6537	0.7547	4
22614	162	10:21:32	39.18	266.15	−0.0520	−0.7733	0.6318	5
22615	162	10:21:40	39.18	266.15	−0.0520	−0.7733	0.6318	6
25247	162	17:11:12	35.7	266.43	−0.0505	−0.8105	0.5835	7
30233	163	10:46:17	26.78	267.1	−0.0452	−0.8915	0.4506	8
33166	164	12:45:26	13.58	267.83	−0.0367	−0.9713	0.2349	9
				Area east of footpad 2				
22044	161	09:29:06	51.8	264.7	−0.0571	−0.6157	0.7859	10
22532	162	10:00:17	39.37	266.2	−0.0512	−0.7714	0.6343	11
30271	163	10:50:17	26.75	267.1	−0.0452	−0.8918	0.4501	12
34005	164	18:51:20	10.43	267.95	−0.0352	−0.9829	0.1811	13
34103	164	19:11:42	10.28	267.97	−0.0349	−0.9833	0.1785	14
				Area west of footpad 2				
00722	153	07:43:09	29.4	91.2	−0.0182	0.8710	0.4909	15
01324	153	09:45:06	30.42	91.5	−0.0226	0.8621	0.5063	16
02151	154	04:09:59	39.78	92.2	−0.0295	0.7679	0.6399	17
07115	155	10:55:18	55.3	94.1	−0.0407	0.5678	0.8221	18
07201	156	06:22:34	65.2	96.5	−0.0475	0.4167	0.9078	19
07225	156	06:41:30	65.38	96.6	−0.0477	0.4137	0.9091	20
10347	156	11:22:35	67.77	97.7	−0.0501	0.3751	0.9256	21
10414	156	11:29:49	67.82	97.7	−0.0504	0.3742	0.8260	22

Table 3. *Surveyor* shadow data

Solution	Item	*SW*, in.	*RF*, deg	*R*, in.	*V*, deg	*S*, in.	X_3, in.	Y_3, in.	Z_3, in.
				Footpad 3 shadow solutions					
1	Footpad 3 gas jet	1.375	5	1.344	5.11	10.599	−59.89	46.14	−17.31
2	Footpad 3 gas jet	1.406	5	1.375	5.11	10.594	−59.89	46.13	−17.31
3	Footpad 3 gas jet	6.125	3.75	4.125	5.56	12.024	−59.82	47.43	−18.09
4	Footpad 3 gas jet	6.219	5	5.50	5.65	11.681	−59.84	47.23	−17.81
5A	Footpad 3 gas jet	1.813	5	1.313	6.90	13.914	−59.77	50.36	−17.79
5B	Leg 3 lock fixture	2.906	5	1.313	11.06	21.180	−57.39	50.38	−17.48
6	Footpad 3 gas jet	1.844	5	1.344	6.86	13.819	−59.78	50.28	−17.73
7A	Footpad 3 gas jet	1.906	5	1.313	7.25	14.464	−59.76	51.32	−17.44
7B	Leg 3 lock fixture	3.156	5	1.313	12.01	22.863	−57.34	52.53	−17.44
8	Leg 3 lock fixture	4.125	5	1.313	15.70	29.685	−57.15	60.46	−17.47
9	Footpad 3, top (position 3)	2.250	5	1.313	8.56	17.131	−64.36	60.44	−17.62
				Footpad 2 shadow solutions					
10A	Footpad 2 gas jet	1.156	5	1.344	4.30	9.225	61.02	45.28	−16.24
10B	Leg 2 TV target	1.75	5	1.344	6.51	13.187	57.75	44.42	−15.66
11A	Footpad 2 gas jet	1.563	5	1.313	5.95	11.537	61.09	48.49	−16.31
11B	Leg 2 lock fixture	2.75	5	1.313	10.47	18.849	59.46	48.54	−16.05
11C	Leg 2 TV target	2.406	5	1.313	9.16	16.910	57.86	49.34	−16.02
12A	Leg 2 lock fixture	4.094	5	1.344	15.23	25.673	59.65	56.89	−15.65
12B	Leg 2 TV target	3.613	5	1.344	13.44	22.973	58.03	56.78	−15.64
13A	Footpad 2, top (position 10)	1.656	5	1.281	6.46	11.149	68.19	55.25	−15.91
13B	Footpad 2 (same) to ridge	0.438	5	1.281	1.70	2.842	67.90	47.09	−14.41
14A	Footpad 2, top (position 10)	1.813	5	1.406	6.44	11.108	68.18	55.22	−15.88
14B	Footpad 2 (same) to ridge	0.469	5	1.406	1.66	2.770	67.89	47.02	−14.39
15	Footpad 2, top (position 3)	0.844	5	0.969	4.35	7.138	69.33	26.78	−17.10
16	Footpad 2, top (position 3)	0.781	5	0.969	4.02	6.632	69.34	27.28	−16.95
17	Footpad 2, top (position 3)	0.844	5	1.313	3.21	5.551	69.36	28.73	−17.15
18	Footpad 2, top (position 3)	0.613	5	1.281	2.39	4.590	69.38	30.39	−17.37
19	Footpad 2, top (position 3)	0.531	5	1.313	2.02	4.187	69.39	31.25	−17.40
20	Footpad 2, top (position 3)	2.063	1.25	1.25	2.06	4.503	69.41	31.13	−17.69
21	Footpad 2, top (position 3)	0.469	5	1.219	1.92	4.068	69.40	31.47	−17.36
22	Footpad 2, top (position 3)	0.531	5	1.25	2.12	4.508	69.42	31.31	−17.77

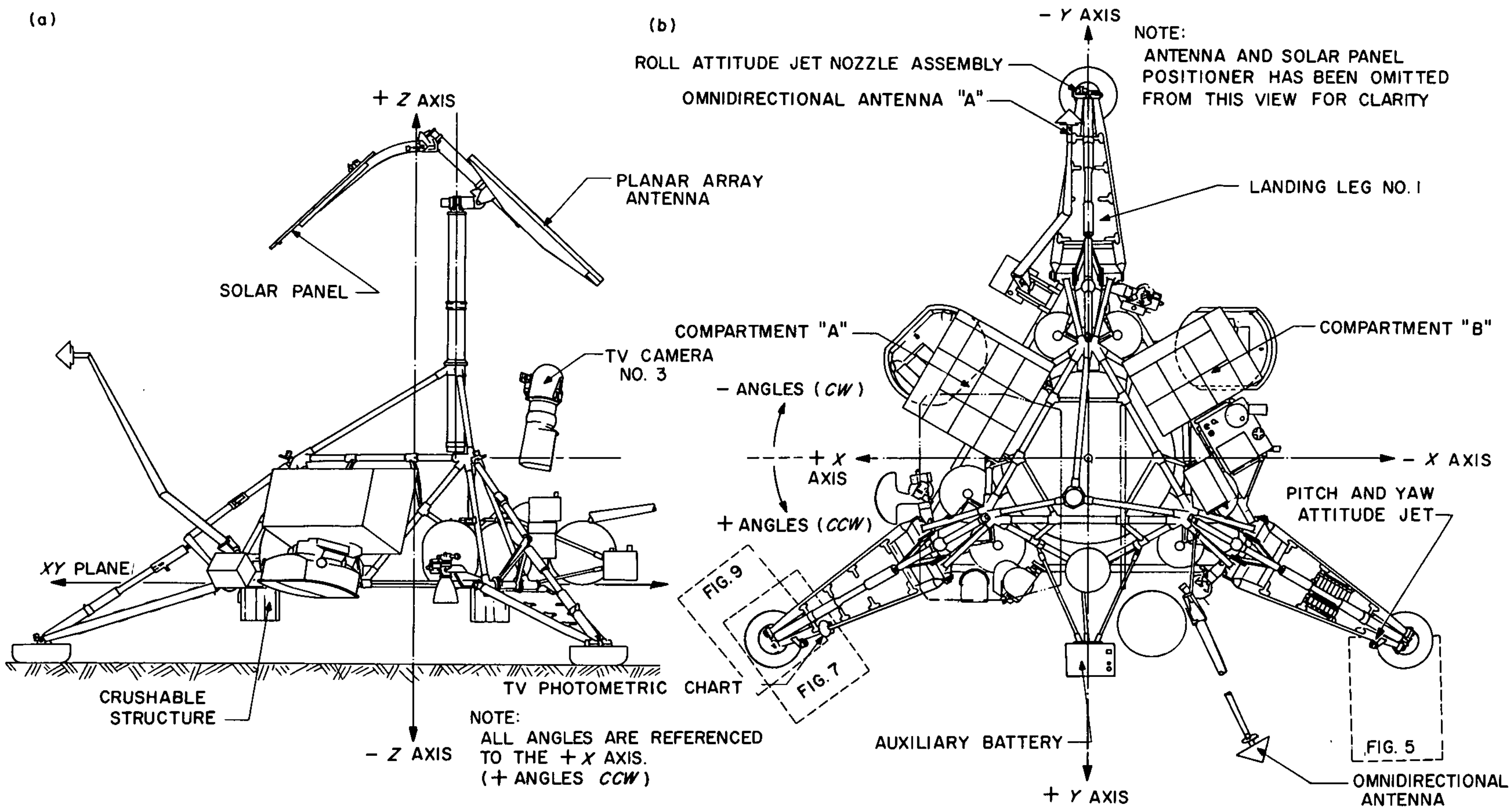

Fig. 4. Modified spacecraft axis system as used in the shadow analysis program

The final results of all the calculations are tabulated in the X_3, Y_3, and Z_3 columns of Table 3. The data points are plotted to show their relative positions, in both the *XY* plane and the vertical profile view, in Figs. 5 through 10. In these figures, outlines of the footpads indicate their position relative to the calculated surface points. As an additional aid in visualizing the area represented by these figures, several of the *Surveyor I* pictures can be studied in Ref. 4. The GMT times and picture numbers for examples of each area are noted in Table 4.

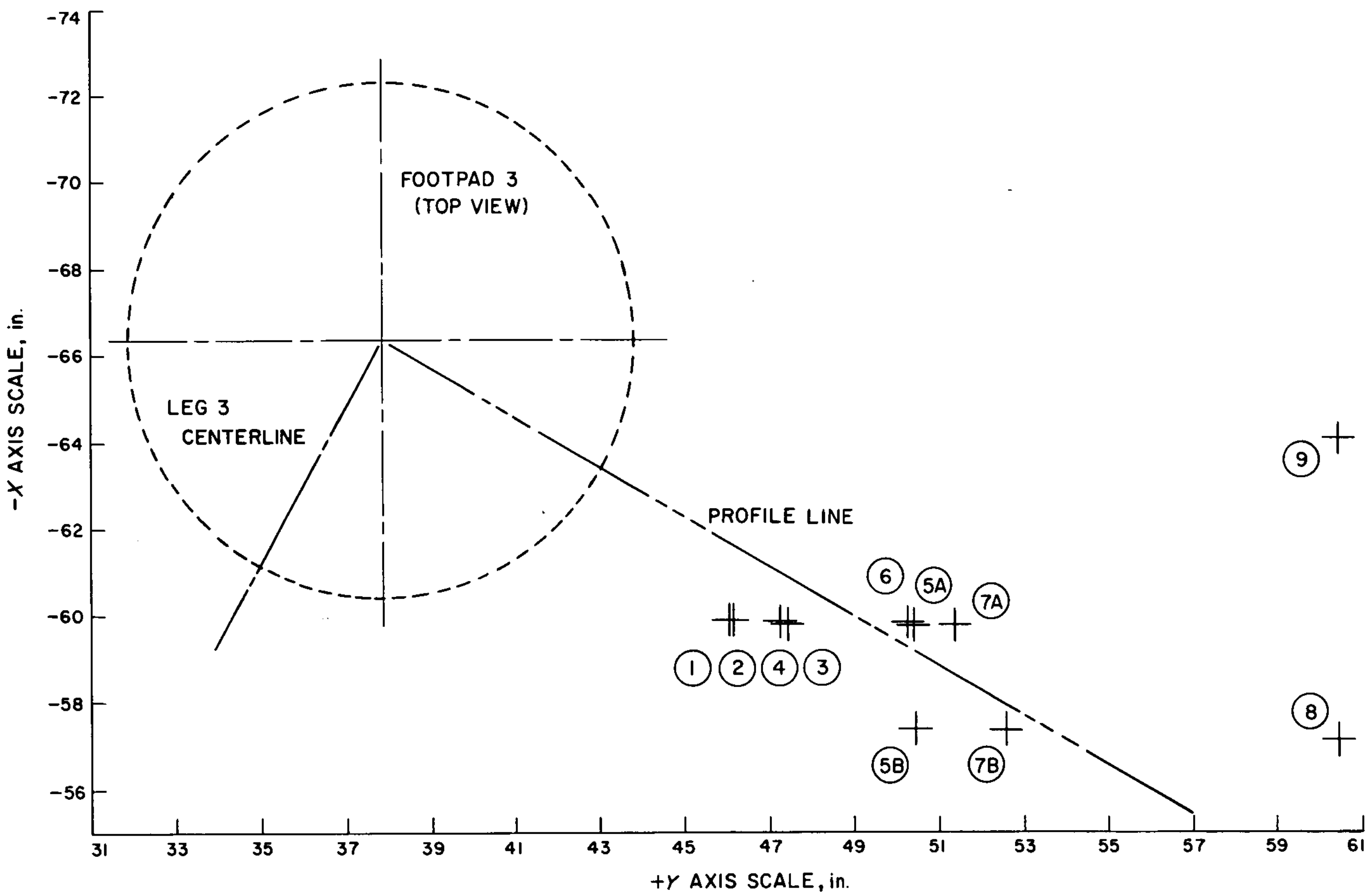

Fig. 5. *Surveyor I* shadow data – XY position of lunar surface points on east side of footpad 3

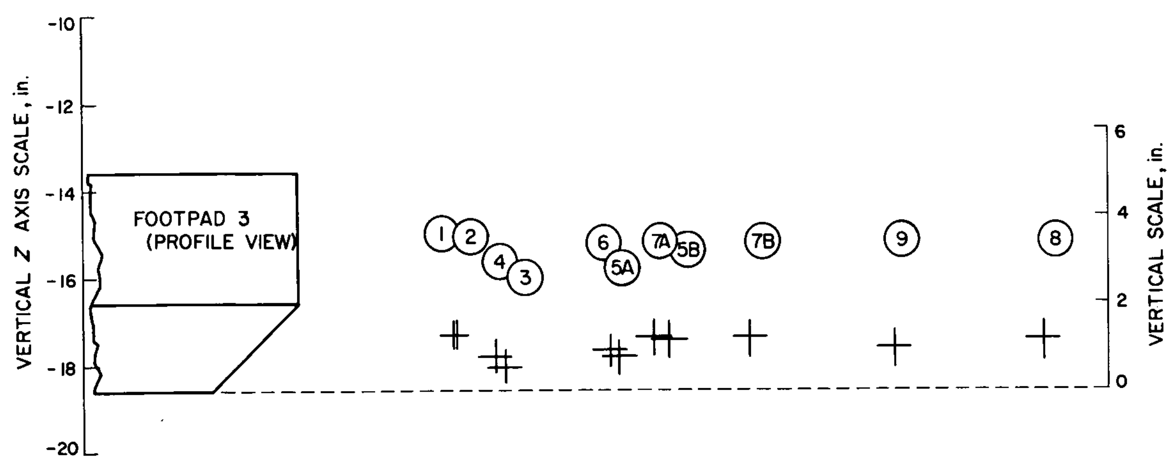

Fig. 6. *Surveyor I* shadow data – profile plot of lunar surface points on east side of footpad 3

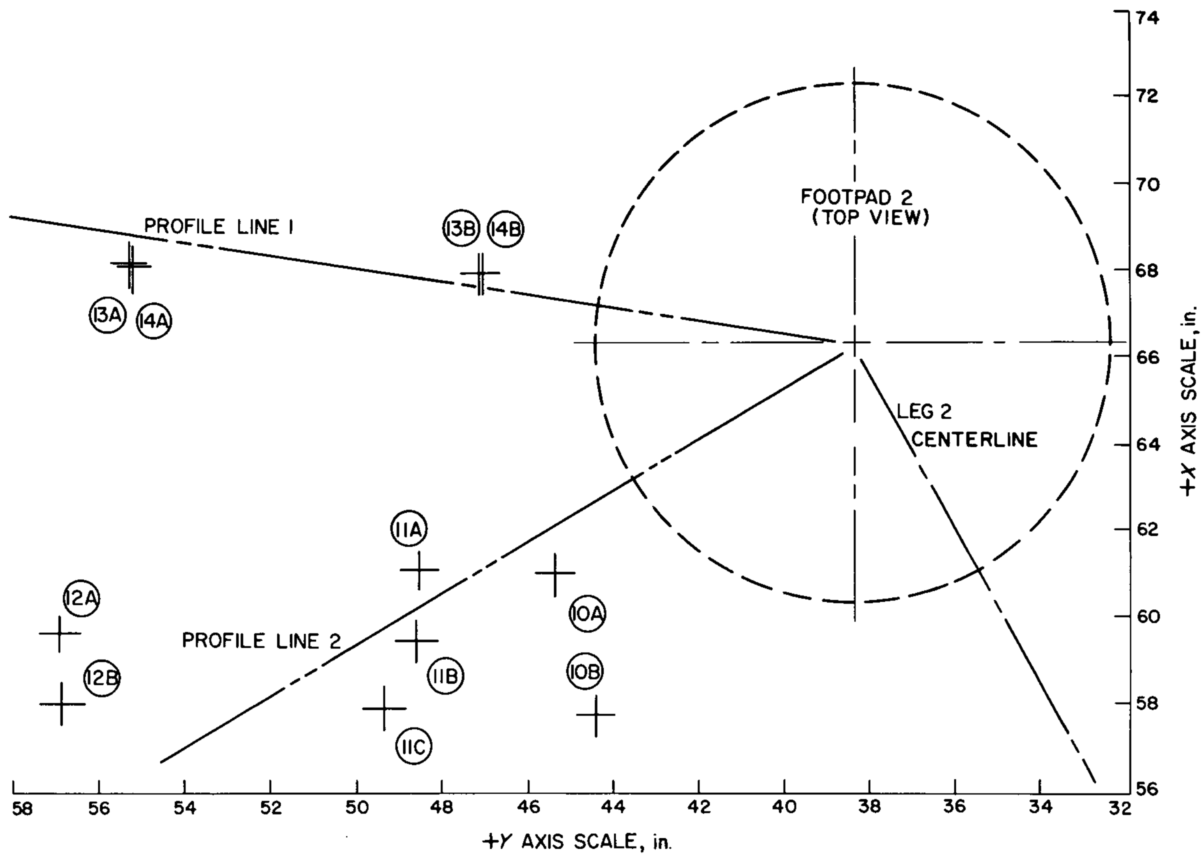

Fig. 7. Surveyor I shadow data – XY position of lunar surface points on east side of footpad 2

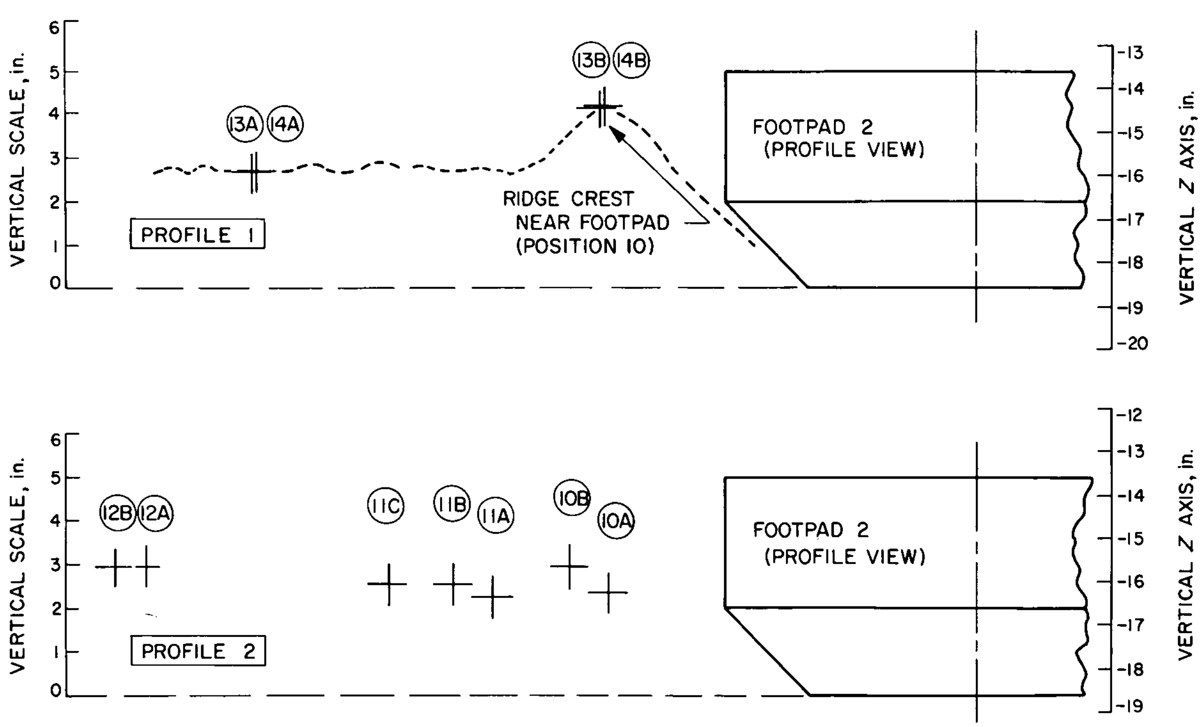

Fig. 8. Surveyor I shadow data – profile plot of lunar surface points on east side of footpad 2

Before discussing the error probabilities, some of the general aspects and implications of these profiles should be considered. The vertical spread of the data points in each group is approximately 1 in. This spread could be caused by random errors in the solutions, actual variations in the vertical positions of the surface points, or a combination of both. Is it reasonable to conclude that the surface granular material in an undisturbed area could have such a large vertical irregularity? Reference 4 presents pictures of the nearby lunar surface taken with the low-angle sunlight of the lunar afternoon. The GMT times and numbers for some of these examples are noted in Table 4. These pictures suggest that the surface is very irregular, and that even larger variations could be considered reasonable.

The general position that is assumed for spacecraft orientation will naturally influence the calculated results.

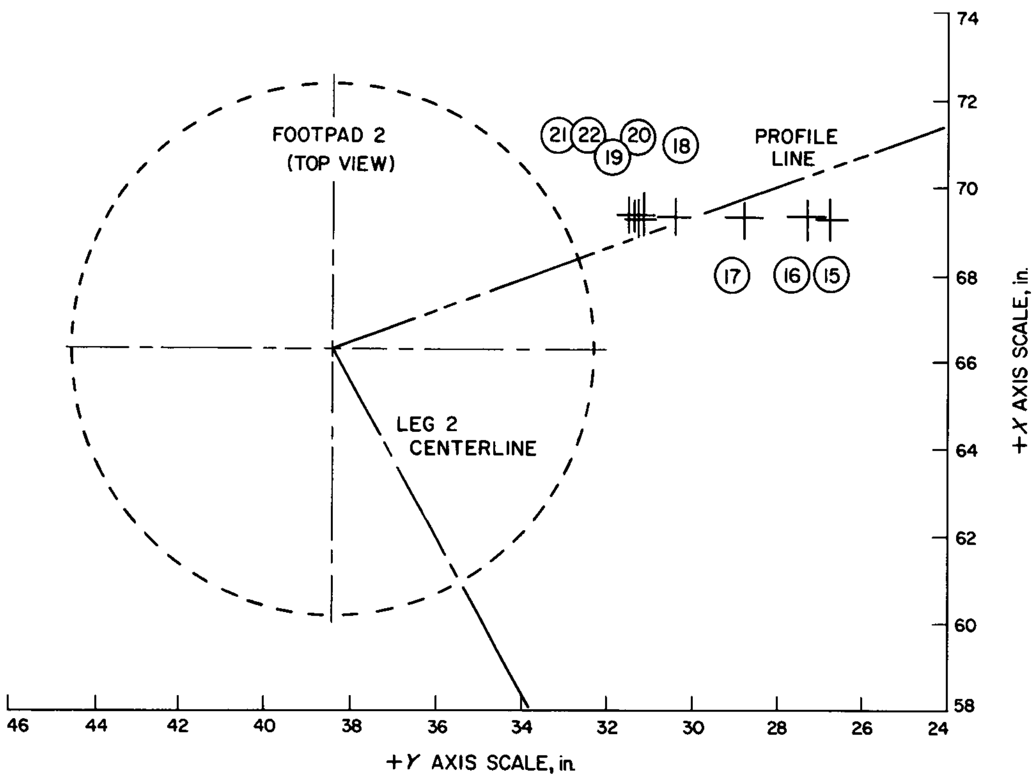

Fig. 9. Surveyor I shadow data – XY position of lunar surface points on west side of footpad 2

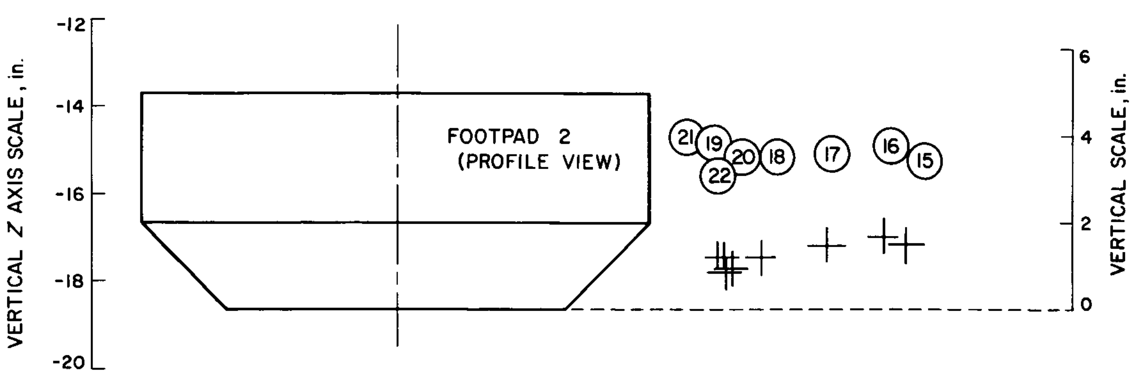

Fig. 10. Surveyor I shadow data – profile plot of lunar surface points on west side of footpad 2

However, the shifts in the assumed position would have to amount to several degrees before they become a problem.

If the landing legs are not resting at an angle of 18 deg, as had been originally assumed, they are probably at a slightly smaller angle. Variations in the leg angle about the nominal 18 deg will change the footpad Z_2 value by the ratio of 0.7 in./deg. For example, reducing leg 3 from 18 to 17 deg would reduce the Z_2 for the footpad top from -13.6 to -12.9 in., or a change of more than 5%. This will cause an equivalent change in Z_3 since it is the sum of Z_2 and the product of $S(\cos\gamma')$. However, the relative position of footpad 3 and the surface points will not change by more than 1.5% because $S(\cos\gamma')$ is less sensitive to changes in Z_2. In other words, the indicated elevation of the surface will be strongly dependent upon the assumed leg angle, but the indicated footpad penetration depth is less dependent on this factor.

Table 4. Reference figures published in *Surveyor* report[a]

Area	Day	Time	Report page	Report figure	Figures used[b]
Footpad 2	153	07:43:10	42	I-3	15
	153	09:45:07	43	I-4	16
	162	10:14:32	107	I-68	
	162	10:25:26	112	I-73	
	162	16:14:15	181	I-142	
	164	11:29:58	200	I-161	
	164	19:11:43	217	I-178	14
	164	(mosaic)	354	(mosaic 29)	
	164	19:44:15	218	I-179	
	164	19:46:35	219	I-180	
Footpad 3	162	17:11:13	182	I-143	7
	163	10:46:17	186	I-147	8
	164	19:02:50	214	I-175	
	164	19:02:57	215	I-176	
	194	(mosaic)	356	(mosaic 31)	
Nearby surface	162	10:20:03	108	I-69	
	163	11:33:05	190	I-151	
	163	11:44:16	192	I-153	
	163	12:48:31	196	I-157	
	163	12:49:58	197	I-158	
	164	11:47:12	201	I-162	
	164	11:51:46	203	I-164	
	164	12:20:32	204	I-165	
	164	19:49:05	222	I-183	
	164	(mosaic)	340	(mosaic 17)	

[a] The TV pictures listed above were obtained from *Surveyor* Mission A and show the lunar surface areas considered in this report. Pictures were published in Ref. 4.

[b] Numbers in this column identify photographs used for the indicated shadow solutions.

V. Error Analysis

The computer program and the IBM 1620 computer were used in the analysis of errors in the shadow solutions. This computer program is described in the appendixes.

The analysis consisted of calculating the magnitude and percentage changes in X_3, Y_3 and Z_3 when the input parameters are varied. The computer program can handle eight different percentage variations, or plus and minus four different levels, for the ten main input parameters. This range of percentage levels was chosen to include the plus and minus values of (A) the smallest measurable increment of each parameter, (B) and (C) two separate choices of the probable input errors (maximum and minimum) for each parameter, and (D) a larger, gross error level which exceeds all probable parameter errors. The computer considers each parameter variation as a separate problem and calculates all outputs. This amounts to 80 problem calculations for each solution. However, the computer completes the total solution in seconds.

The computer prints out the results of all these error calculations as columns of percentages and final values for X_3, Y_3, and Z_3. The final step of selecting a combination of ten output errors (one for each parameter at the chosen input error level) and calculating the RMS or algebraic sum of the individual errors, is left as a manual calculation for the investigator.

The computer program could be refined by including the calculation of the combined RMS errors. However, this would require the selection of a particular set of individual error percentages that could be applied to all solutions. At this time, the range of possible values has not been narrowed sufficiently to mechanize this step.

A shadow solution was selected from each of the areas under consideration to demonstrate the application of the computer error analysis. The resulting printouts are included in Appendix C. Solution 8 was east of footpad 3, solution 10A was east of footpad 2, and solution 15 was west of footpad 2.

The input parameter variations picked for these computer error solutions are listed in Table 5. The calculated output errors are unique to these solutions and could not be generally applied to all shadow problems. However, they indicate the relative effects of each input parameter and the error sensitivity slope as the percentage is increased.

Table 5. Input parameter variations for error analysis

Parameter	Symbol	± Percentage increments[a]			
		(A)	(B)	(C)	(D)
Sun elevation angle	θ	0.2	0.4	1	2
Sun azimuth angle	ϕ	0.1	0.2	0.5	2
Reseau scale	R	0.5	1.0	2	5
Shadow length	SW	0.5	1.0	2	5
S/C measurements	$X_1X_2Y_1Y_2Z_1Z_2$	0.2	0.5	1	5

[a] The percentage values chosen for each parameter are representative of:
(A) The smallest increment that can be easily measured.
(B) The probable error level (minimum range).
(C) The probable error level (maximum range).
(D) A large error level to indicate gross effects on output.

Table 6. Results of computer error analysis

Output parameter	RMS total errors in each range							
	(A)		(B)		(C)		(D)	
	%	in.	%	in.	%	in.	%	in.
Solution 8								
X_3	0.29	0.17	0.66	0.38	1.5	0.84	6.7	3.8
Y_3	0.40	0.24	0.83	0.50	1.7	1.03	5.6	3.4
Z_3	0.67	0.12	1.36	0.24	2.8	0.50	8.2	1.4
Solution 10A								
X_3	0.20	0.12	0.50	0.31	1.02	0.62	5.05	3.1
Y_3	0.22	0.10	0.52	0.24	1.04	0.47	4.91	2.2
Z_3	0.41	0.07	0.86	0.14	1.81	0.29	6.13	0.99
Solution 15								
X_3	0.20	0.14	0.50	0.35	1.0	0.70	5.0	3.5
Y_3	0.31	0.08	0.72	0.19	1.4	0.39	6.6	1.8
Z_3	0.23	0.04	0.52	0.09	1.1	0.18	4.5	0.76

Table 6 presents a summary of the total RMS errors for these three shadow solutions. Each of the four percentage columns were calculated as a separate RMS total to indicate how each level of input errors can affect the final output results. In a typical error analysis, only one RMS total would be needed.

The effect of errors in the angle of the landing legs could be included as part of the $X_2Y_2Z_2$ increments; however, it would be better to keep the angle as a separate error input. As previously mentioned, the effect on Z_2 is about 0.7 in./deg change; however, this is a fixed bias on all solutions that will cause a common shift in all the Z_3 levels. Therefore, this bias error must be remembered although it is not specifically included in every total.

VI. Conclusions and Potential Applications

The application of the shadow analysis to some typical *Surveyor* Mission A data was demonstrated by the 30 shadow solutions and the 3 error calculations. The calculated lunar surface elevations are plotted in Figs. 5 through 10. The penetration depth of the footpads is indicated by the relative position of the pads in the profile views.

Some important limitations in measuring actual footpad penetration should be pointed out. At best, the analysis is an attempt to determine the final resting position of the footpads and not the maximum penetration that occurred during the first landing contact. The closest shadow data points are still inches away from the edge of the footpads, so that penetration numbers are relative to the nearby surface and not to the actual soil under the pads.

With these limitations in mind, some probable conclusions about footpad penetration can be considered. The data profile in Fig. 6 would indicate an average penetration of 1 in. for footpad 3. Figure 8 shows a partial profile through part of the ridge thrown up by footpad 2. The data profiles in Figs. 8 and 10 suggest penetration values of from 0.8 to 3 in. for footpad 2. Would it have been even possible for footpads 2 and 3 to have penetrations as different as 3 to 1? Studies of the *Surveyor I* strain gauge data and landing dynamics by F. B. Sperling of JPL have ruled out this possibility. A large difference in penetration depth could be expected to produce noticeably different leg force levels. The strain gauge data indicate similar loads in all three legs (Ref. 5).

Therefore, it can be concluded that the data profile from the west side of footpad 2 (Fig. 10) is more indicative of the actual penetration of this pad. This is in the 0.8- to 1.6-in. range. In this case, the difference between the two profiles, east and west of the pad, would indicate an actual difference in elevation, because of a shallow crater or rise. Again, a visual study of some of the *Surveyor I* pictures, as noted for footpad 2 in Table 4, can give a better understanding of the situation. Figures I-179 and I-180 (pp. 218 and 219, Ref. 4) would particularly be helpful in determining, by visual interpretation, the presence of a shallow depression in the area to the southwest of footpad 2. Mosaic 29 (p. 354, Ref. 4), combines these photographs and increases the perception of a depression. The pictures showing the east side are not as clear or as well lighted; however, the presence of a higher area seems a reasonable interpretation.

Some additional work would be necessary to explain the situation around footpad 2; however, the data support the conclusion that there is a significant variation in the surface elevation around the pad. However, there is still considerable doubt about the original level of the material directly under the footpad. It may have had a sloping surface. At present, it could be speculated that footpad 2 impacted in an area of slightly lower elevation and came to rest in contact with the eastern boundary of this area.

The computer program presented in Appendix B reduces the time required for calculations and data conversion to a minimum, and makes it possible to run many solutions rapidly. The material presented in the main part of this report plus the appendix should be sufficient to assist interested investigators in conducting analyses of similar data. The shadow analysis method is suggested as a possible tool for photographic data reduction.

There are still hundreds of photographs from *Surveyor* Mission A, not considered in this report, that could be used for additional shadow analysis work. Similar pictures from *Surveyor* Missions C through G could also be analyzed by this method.

For a more complete analysis of the footpad interaction with the lunar surface, E. Christensen of JPL has proposed attaching several thin radial rods or whiskers to the tops of footpads 2 and 3. These rods would cast shadows on the surface area adjacent to the footpads. The shadow analysis method would then make it possible (1) to draw cross-section profiles through the disturbed material ridge pushed up by the footpad, (2) to construct such disturbed material profiles on two, and maybe three, sides of the footpad, and (3) to determine footpad penetration relative to the material immediately adjacent to the footpad. This relatively small investment could produce a bonanza of useful scientific data. The shadow analysis program would be directly applicable for the reduction of photographic data of such whisker-type devices.

The computer program, the printout of the complete program, and the tabulated printout for the several computer solutions are discussed in Appendixes A, B, and C.

References

1. *Attitude Matrix and Sun/Earth Positions,* Interdepartmental Correspondence, 2292/20, SC-10, Hughes Aircraft Company, El Segundo, Calif., Aug. 19, 1966.

2. *Scientific Data and Results, Surveyor I* Mission Report, Part II. Technical Report 32-1023, Jet Propulsion Laboratory, Pasadena, Calif., 1966.

3. *Surveyor Spacecraft A-21 Configuration,* Drawing 276806A (J-size edition), Hughes Aircraft Company, El Segundo, Calif.

4. *Television Data, Surveyor I* Mission Report, Part III. Technical Report 32-1023, Jet Propulsion Laboratory, Pasadena, Calif., 1966.

5. Sperling, F. B., and Garba, J. A., *A Description of the Surveyor Lunar Landing Dynamics and an Evaluation of Pertinent Telemetry Data Returned by Surveyor I.* Technical Report 32-1035, Jet Propulsion Laboratory, Pasadena, Calif., 1967.

Appendix A
Computer Program for *Surveyor* Shadow Analysis

I. Introduction

To reduce the time and effort required for the calculation of shadow solutions and probable errors, a computer program was prepared by L. I. Busch, JPL's Section 314 (Computation and Analysis Section). The program, in FORTRAN II language, was written for the IBM 1620 (Monitor II) computer. The program can be also converted for the IBM 7094 computer.

The symbols, nomenclature, and calculations used in the computer analysis are the same as discussed previously and are summarized on the following pages. The methods for determining the various data input items are discussed in the main sections of this report.

A complete printout of the computer program is presented in Appendix B. This consists of the error analysis subroutine, which is read into the computer memory disc for semi-permanent storage, and the main shadow analysis program, which must be used with each batch of shadow calculations. Once the error analysis has been stored, it can be recalled by the computer whenever needed. The inclusion of the error analysis is an optional choice that is made at the time of each data run. The format that must be used in preparing data input cards is also illustrated in Appendix B. A total of 245 cards, plus 2 cards for each solution input, are used.

Appendix C presents the computer printout for *Surveyor I* shadow solutions 8, 10A, and 15. All input parameters and the calculation results are listed in these printouts. The error analysis then gives the output percentage changes and the new output values resulting from each input parameter change. The total error effects can then be obtained by combining a set of these individual parameter errors. The investigator is free to make his own choice of the most probable error magnitude for each parameter and to use addition or RMS summation of the combination. A list of RMS error calculations for these three solutions is given in Table 6.

The computer program can be used for the analysis of *Surveyor* shadow data or of any similar photographic data, assuming that the characteristics and limitations of this approach are fully considered. Although the dimensional unit of inches was used for the calculations, other units, such as metric units, could be used if they are kept consistent throughout a solution.

II. *Surveyor* Shadow Analysis

A. Inputs

Symbol	
$X_1 Y_1 Z_1$	location of a point in space within an XYZ axis system
$X_2 Y_2 Z_2$	location of other points in the XYZ axis system (described by I.D. below)
L_p	distance from elevation mirror pivot axis to TV camera front nodal point
I.D.	identification of item located at $X_2Y_2Z_2$
GMT	GMT time (hr-min-sec)
θ	sun elevation angle above XY plane
ϕ	sun azimuth angle, from $+X$ axis
R	reseau mark spacing width
RF	reseau reference angle
SW	length of shadow view line

B. Outputs and Other Parameters

$X_p Y_p Z_p$	location of TV camera *front nodal point* for the camera azimuth, elevation and focal length being considered
$X_3 Y_3 Z_3$	location of a point in XYZ axis system
S	length of shadow
L	length of line from $X_1Y_1Z_1$ to each $X_2Y_2Z_2$
cos of $\alpha\ \beta\ \gamma$	direction cosine angles from line L to XYZ axes
cos of $\alpha'\ \beta'\ \gamma'$	direction cosines of sun line to XYZ axes
N	intersect angle between line L and sun line
cos N	cosine of angle N
Angles V and D	V is shadow view angle (angles V, D, and N form triangle)

Calculations

$$\text{angle}\,(V) = \frac{(RF)\,(SW)}{(R)} \qquad (1)$$

$$L = [(X_2 - X_1)^2 + (Y_2 - Y_1)^2 + (Z_2 - Z_1)^2]^{1/2} \qquad (2)$$

$$\cos\alpha = \frac{X_2 - X_1}{L} \qquad (3)$$

$$\cos\beta = \frac{Y_2 - Y_1}{L} \qquad (4)$$

$$\cos\gamma = \frac{Z_2 - Z_1}{L} \qquad (5)$$

$$X_p = (\cos\alpha)\,(L + L_p) - X_2 \qquad (6)$$

$$Y_p = (\cos\beta)\,(L + L_p) - Y_2 \qquad (7)$$

$$Z_p = (\cos\gamma)\,(L + L_p) - Z_2 \qquad (8)$$

$$\cos\alpha' = \cos\theta\cos\phi \qquad (9)$$

$$\cos\beta' = \cos\theta\sin\phi \qquad (10)$$

$$\cos\gamma' = \sin\theta \qquad (11)$$

$$\cos(N) = \cos\alpha\cos\alpha' + \cos\beta\cos\beta' + \cos\gamma\cos\gamma' \qquad (12)$$

$$\text{Angle}\,(D) = \pi - (N + V) \qquad (13)$$

$$S = \frac{(L + L_p)\,(\sin V)}{(\sin D)} \qquad (14)$$

$$X_3 = X_2 - S\cos\alpha' \qquad (15)$$

$$Y_3 = Y_2 - S\cos\beta' \qquad (16)$$

$$Z_3 = Z_2 - S\cos\gamma' \qquad (17)$$

Appendix B
Computer Program

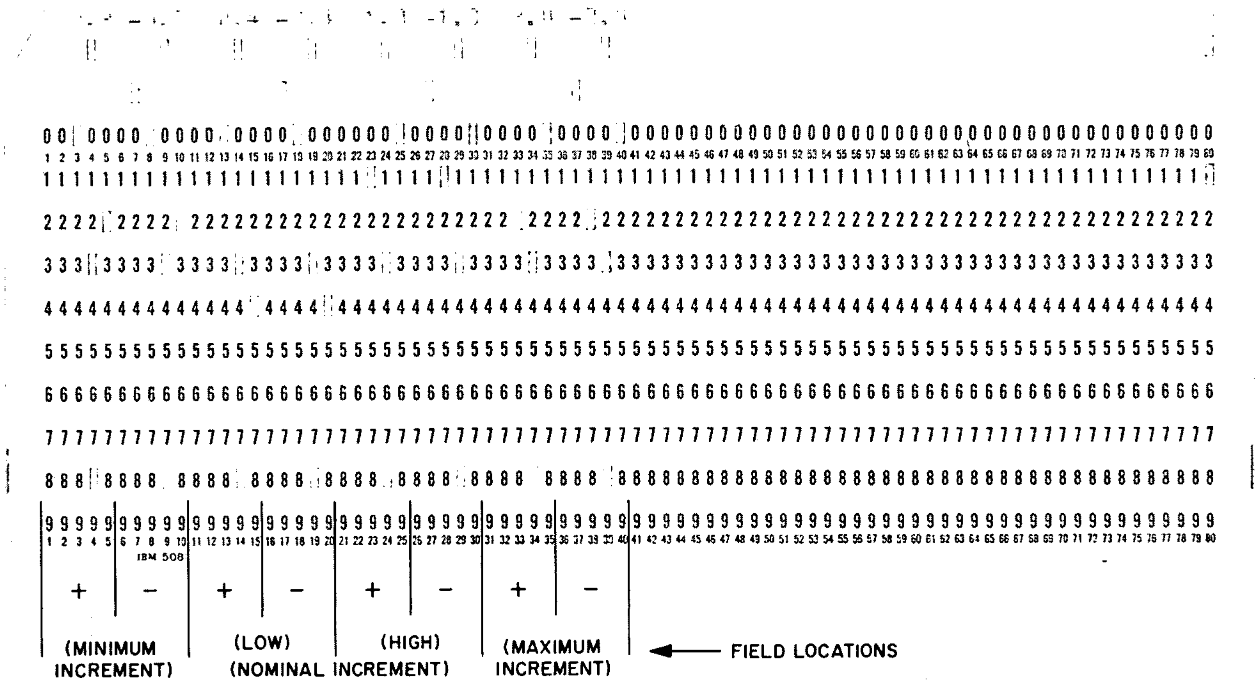

CARD	PARAMETER
A	θ (SUN EL)
B	ϕ (SUN AZ)
C	R (RESEAU)
D	SW (SHADOW)
E	X_1
F	X_2
G	Y_1
H	Y_2
I	Z_1
J	Z_2

DATA CARD 1

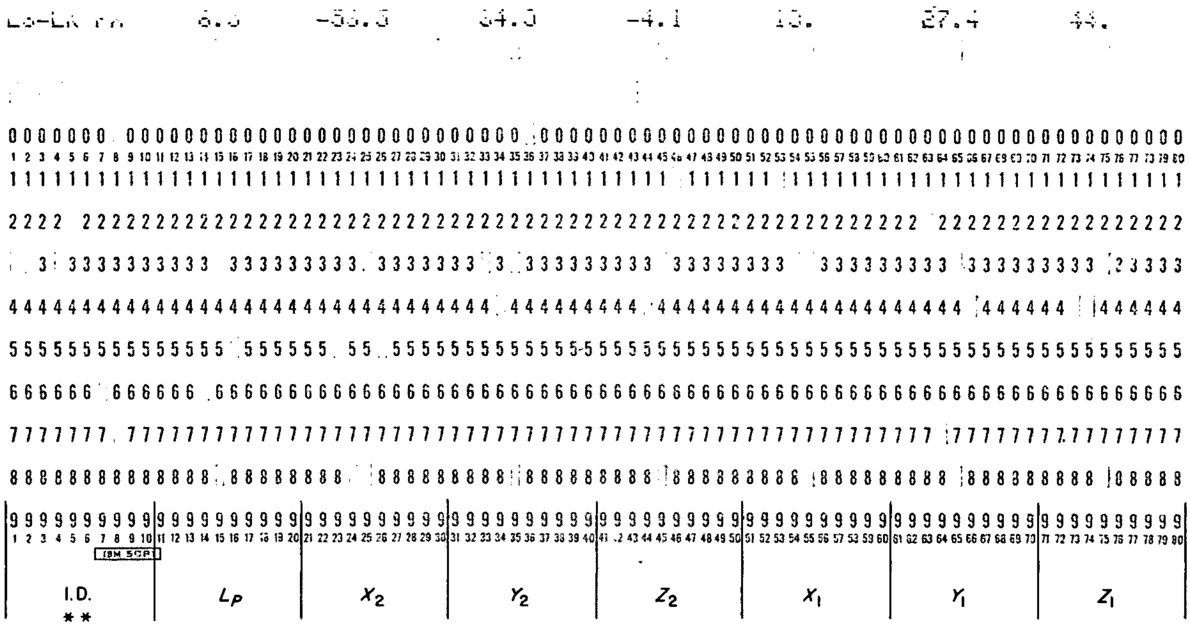

(FIELD LOCATIONS)

DATA CARD 2

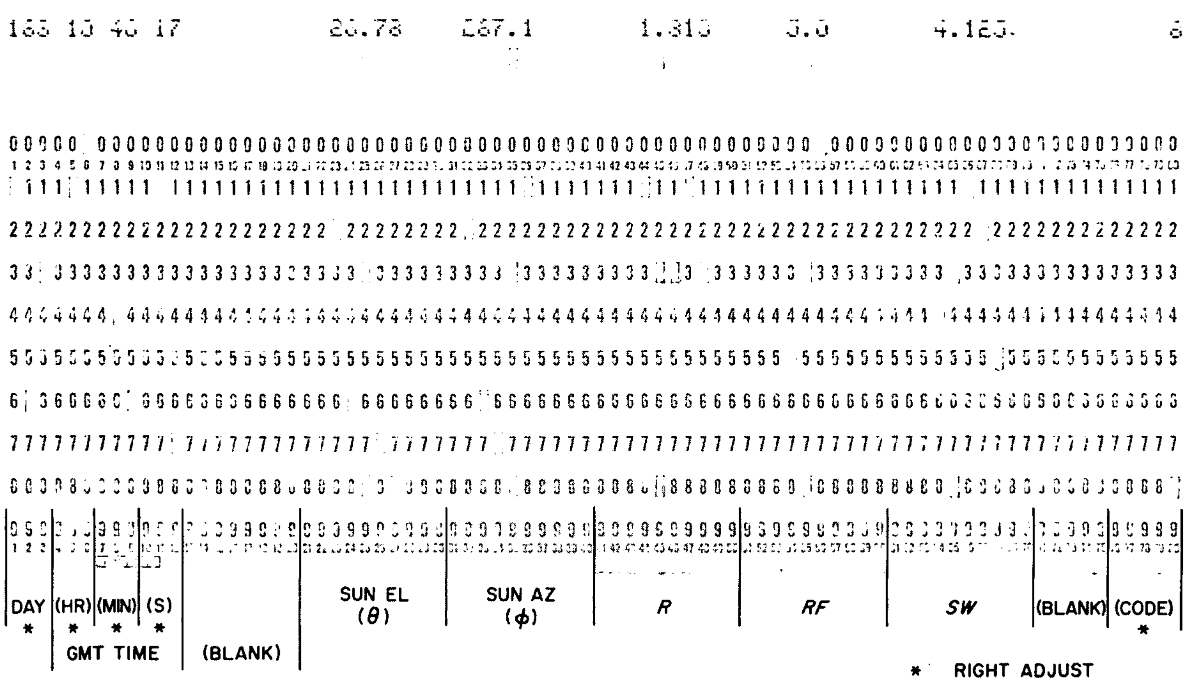

* RIGHT ADJUST

** LEFT ADJUST

```
C       IBM 1620 (MONITOR II SYSTEM) PROGRAM FOR SURVEYOR SHADOW ANALYSIS
C       ERROR ANALYSIS IS OPTIONAL
C
C       FORMAT OF INPUT...
C         CARDS A THROUGH J..CONSTANTS FOR ERROR ANALYSIS...(8F5.0)
C         CARD 1..ID,LP,X2,Y2,Z2,X1,Y1,Z1...(10A1,7F10.0)
C         CARD 2..DAY,HR,MIN,SEC,THETA,PHI,R,RF,SW,CODE...
C                                           (4I3,8X,5F10.0,5X,5A1)
C       NOTE..CARDS A THROUGH J WILL ALWAYS BE READ IN FIRST.
C           ..CARDS 1 AND 2 WILL BE REPEATED FOR EACH NEW CASE.
C
C       DESCRIPTION OF INPUT...
C         ERROR ANALYSIS CONSTANTS (INCREMENTS IN PERCENT FOR THETA,PHI,R,
C                                SW,X1,X2,Y1,Y2,Z1,Z2)
C         ID (IDENTIFICATION OF ITEM LOCATED AT X2,Y2,Z2)
C         LP(DISTANCE OF TV CAMERA FRONT NODAL POINT FROM ELEVATION
C             MIRROR PIVOT AXIS)
C         X1,Y1,Z1 (LOCATION OF A POINT IN SPACE WITHIN XYZ AXIS SYSTEM)
C         X2,Y2,Z2 (LOCATION OF OTHER POINTS IN XYZ AXIS SYSTEM,
C                   DESCRIBED BY ID)
C         GMT (GREENWICH MEAN TIME..DAY,HOURS,MINUTES,SECONDS)
C         THETA (SUN ELEVATION ANGLE ABOVE X,Y PLANE)
C         PHI (SUN AZIMUTH ANGLE,FROM +X AXIS)
C         R (RESEAU MARK SPACING WIDTH)
C         RF (RESEAU REFERENCE ANGLE)
C         SW (LENGTH OF SHADOW VIEW LINE)
C         CODE (IDENTIFICATION OF MISSION AND POINT IN MISSION)
C               (I.E. 27A WOULD INDICATE POINT 27 OF MISSION A)
C
C       OUTPUT...MAIN PROGRAM...
C         INPUT PARAMETERS AND IDENTIFICATION
C         L (LENGTH OF LINE FROM X1,Y1,Z1 TO X2,Y2,Z2)
C         N (INTERSECT ANGLE BETWEEN LINE L AND SUN LINE)
C         D (PI - (N+V))
C         V ( (RESEAU REF.)(SHADOW ANGLE)/(RESEAU SCALE) )
C         S (LENGTH OF SHADOW)
C         X3,Y3,Z3 (LOCATION OF A POINT IN XYZ AXIS SYSTEM)
C         LP (DIST. FROM TV FRONT NODAL POINT TO EL. MIRROR (X1,Y1,Z1))
C         XP,YP,ZP (LOCATION OF FNP)
C
C       OUTPUT...ERROR ANALYSIS (OPTIONAL)
C         VARYING PARAMETER (THETA,PHI,R,SW,X1,X2,Y1,Y2,Z1, OR Z2)
C         PERCENTAGE CHANGE IN X3,Y3,Z3 FROM NOMINAL WITH VARIATION OF
C                           ONE PARAMETER,WHILE ALL OTHERS REMAIN CONSTANT
C         NEW VALUES OF X3,Y3,Z3
C
C       NOTE...EXECUTION OF PROGRAM WILL PAUSE TO PERMIT SELECTION OF
C              OPTION OF MAIN PROGRAM ONLY OR MAIN PROGRAM+ ERROR ANALYSIS
C           ...MOVE SENSE SWITCH 3 TO ON POSITION IF ERROR ANALYSIS
C              IS DESIRED
C
C
C       SURVEYOR SHADOW ANALYSIS CALCULATIONS...R.L.SPENCER,(LIB,2/67)
      4 FORMAT(1H1,38X29HSURVEYOR SHADOW ANALYSIS DATA,//)
      5 FORMAT(7X3HGMT,21X3HSUN,/1X3HDAY,2X2HHR,1X3HMIN,1X3HSEC,7X9HEL(THE
       1TA),2X7HAZ(PHI),12X1HR,9X2HRF,8X2HSW)
      6 FORMAT(4I4,F15.2,F10.2,F16.5,F10.2,F10.4,38X,5A1,/)
      7 FORMAT(27X,2HID,24X2HX2,8X2HY2,8X2HZ2,10X2HX1,8X2HY1,8X2HZ1,/23X
       1 10A1,14X3F10.2,2X3F10.2,/)
```

```
  8 FORMAT(26X1HL,9X1HN,9X1HD,9X1HV,9X1HS,18X2HX3,8X2HY3,8X2HZ3,/19X
   1 4F10.2,F11.3,9X3F10.2,/)
 10 FORMAT(10A1,7F10.0)
 11 FORMAT(4I3,8X5F10.0,5X5A1)
 12 FORMAT(76HIF ERROR ANALYSIS IS DESIRED,PUT SENSE SWITCH 3 ON,AND P
   1USH START ON CONSOLE/ 23HIF NOT,JUST PUSH START.)
 13 FORMAT(8F5.0)
 14 FORMAT(25X2HLP,58X2HXP,8X2HYP,8X2HZP,/19XF10.2,50X3F10.2,//)
C
    DIMENSION ID(10),CODE(5),THETAE(8),PHIE(8),RE(8),SWE(8),X1E(8),
   1 Y1E(8),Z1E(8),X2E(8),Y2E(8),Z2E(8)
    COMMON THETAE,PHIE,RE,SWE,X1E,Y1E,Z1E,X2E,Y2E,Z2E,CONVF,ELP
    CONVF=.01745329
    READ 13,THETAE,PHIE,RE,SWE,X1E,Y1E,Z1E,X2E,Y2E,Z2E
 15 PRINT 4
    TYPE 12
    PAUSE
  1 READ 10,ID,ELP,X2,Y2,Z2,X1,Y1,Z1
    READ 11,IDAY,IHR,MIN,ISEC,THETA,PHI,R,RF,SW,CODE
    EL=SQRT((X2-X1)**2+(Y2-Y1)**2+(Z2-Z1)**2)
    COSA=(X2-X1)/EL
    COSB=(Y2-Y1)/EL
    COSG=(Z2-Z1)/EL
    XP=X2-COSA*(EL+ELP)
    YP=Y2-COSB*(EL+ELP)
    ZP=Z2-COSG*(EL+ELP)
    COSTH=COS(THETA*CONVF)
    SINTH=SIN(THETA*CONVF)
    COSPH=COS(PHI*CONVF)
    SINPH=SIN(PHI*CONVF)
    V=(RF*SW)/R
    SINV=SIN(V*CONVF)
    COSAP=COSTH*COSPH
    COSBP=COSTH*SINPH
    COSGP=SINTH
    COSN=COSA*COSAP + COSB*COSBP + COSG*COSGP
    EN=ATAN(SQRT(1.0-COSN**2)/COSN)*57.29578 + 180.0
    D=180.0-EN-V
    SIND=SIN(D*CONVF)
    S=(EL+ELP)*SINV/SIND
    X3=X2-S*COSAP
    Y3=Y2-S*COSBP
    Z3=Z2-S*COSGP
    PRINT 5
    PRINT 6,IDAY,IHR,MIN,ISEC,THETA,PHI,R,RF,SW,CODE
    PRINT 7,ID,X2,Y2,Z2,X1,Y1,Z1
    PRINT 8,EL,EN,D,V,S,X3,Y3,Z3
    PRINT 14,ELP,XP,YP,ZP
    IF(SENSE SWITCH 3)2,3
  2 CALL ERRAN(THETA,PHI,R,SW,RF,X1,Y1,Z1,X2,Y2,Z2,X3,Y3,Z3)
  3 IF(SENSE SWITCH 3)15,1
    END
```

I. Sample Format of Input, Cards A–J, Percentage Increments for Error Analysis

```
*LDISK
      SUBROUTINE ERRAN(THETA,PHI,R,SW,RF,X1,Y1,Z1,X2,Y2,Z2,X3,Y3,Z3)
      DIMENSION THETAE(8),PHIE(8),RE(8),SWE(8),X1E(8),Y1E(8),Z1E(8),
     1 X2E(8),Y2E(8),Z2E(8)
      COMMON THETAE,PHIE,RE,SWE,X1E,Y1E,Z1E,X2E,Y2E,Z2E,CONVF,ELP
C
   20 FORMAT(1H0,8X14HERROR ANALYSIS,6X17HVARYING PARAMETER,8X20HPERCENT
     1AGE CHANGE IN,16X13HNEW VALUES OF/53X2HX3,8X2HY3,8X2HZ3,10X2HX3,8X
     2 2HY3,8X2HZ3)
   90 FORMAT(31X5HTHETA,F6.2,4H PC ,3F10.3,3X3F10.3)
   91 FORMAT(31X5HPHI  ,F6.2,4H PC ,3F10.3,3X3F10.3)
   92 FORMAT(31X5HR    ,F6.2,4H PC ,3F10.3,3X3F10.3)
   93 FORMAT(31X5HSW   ,F6.2,4H PC ,3F10.3,3X3F10.3)
   94 FORMAT(31X5HX1   ,F6.2,4H PC ,3F10.3,3X3F10.3)
   95 FORMAT(31X5HX2   ,F6.2,4H PC ,3F10.3,3X3F10.3)
   96 FORMAT(31X5HY1   ,F6.2,4H PC ,3F10.3,3X3F10.3)
   97 FORMAT(31X5HY2   ,F6.2,4H PC ,3F10.3,3X3F10.3)
   98 FORMAT(31X5HZ1   ,F6.2,4H PC ,3F10.3,3X3F10.3)
   99 FORMAT(31X5HZ2   ,F6.2,4H PC ,3F10.3,3X3F10.3)
C
      PRINT 20
      THETAO=THETA
      PHIO=PHI
      RO=R
      SWO=SW
      X1O=X1
      Y1O=Y1
      Z1O=Z1
      X2O=X2
      Y2O=Y2
      Z2O=Z2
      X3O=X3
      Y3O=Y3
      Z3O=Z3
      K=0
  100 K=K+1
      I=0
  105 I=I+1
      IF(I-8)107,107,100
  107 GO TO(110,120,130,140,150,160,170,180,190,200),K
  110 THETA=THETA+.01*THETAE(I)*THETA
      GO TO 205
  120 PHI=PHI+.01*PHIE(I)*PHI
      GO TO 205
  130 R=R+.01*RE(I)*R
      GO TO 205
  140 SW=SW+.01*SWE(I)*SW
      GO TO 205
  150 X1=X1+.01*X1E(I)*X1
      GO TO 205
  160 X2=X2+.01*X2E(I)*X2
      GO TO 205
  170 Y1=Y1+.01*Y1E(I)*Y1
      GO TO 205
  180 Y2=Y2+.01*Y2E(I)*Y2
      GO TO 205
  190 Z1=Z1+.01*Z1E(I)*Z1
      GO TO 205
  200 Z2=Z2+.01*Z2E(I)*Z2
C
  205 EL=SQRT((X2-X1)**2+(Y2-Y1)**2+(Z2-Z1)**2)
```

II. Sample Format of Input—Two Cards Required for each Set of Data

```
      COSA=(X2-X1)/EL
      COSB=(Y2-Y1)/EL
      COSG=(Z2-Z1)/EL
      XP=COSA*(EL+ELP)-X2
      YP=COSB*(EL+ELP)-Y2
      ZP=COSG*(EL+ELP)-Z2
      COSTH=COS(THETA*CONVF)
      SINTH=SIN(THETA*CONVF)
      COSPH=COS(PHI*CONVF)
      SINPH=SIN(PHI*CONVF)
      V=(RF*SW)/R
      SINV=SIN(V*CONVF)
      COSAP=COSTH*COSPH
      COSBP=COSTH*SINPH
      COSGP=SINTH
      COSN=COSA*COSAP + COSB*COSBP + COSG*COSGP
      EN=ATAN(SQRT(1.0-COSN**2)/COSN)*57.29578 + 180.0
      D=180.0-EN-V
      SIND=SIN(D*CONVF)
      S=(EL+ELP)*SINV/SIND
      X3=X2-S*COSAP
      Y3=Y2-S*COSBP
      Z3=Z2-S*COSGP
      X3C=(X3/X30)*100.0-100.0
      Y3C=(Y3/Y30)*100.0-100.0
      Z3C=(Z3/Z30)*100.0-100.0
C
      GO TO(210,220,230,240,250,260,270,280,290,300),K
  210 THETA=THETAO
      PRINT 90,THETAE(I),X3C,Y3C,Z3C,X3,Y3,Z3
      GO TO 105
  220 PHI=PHIO
      PRINT 91,PHIE(I),X3C,Y3C,Z3C,X3,Y3,Z3
      GO TO 105
  230 R=RO
      PRINT 92,RE(I),X3C,Y3C,Z3C,X3,Y3,Z3
      GO TO 105
  240 SW=SWO
      PRINT 93,SWE(I),X3C,Y3C,Z3C,X3,Y3,Z3
      GO TO 105
  250 X1=X10
      PRINT 94,X1E(I),X3C,Y3C,Z3C,X3,Y3,Z3
      GO TO 105
  260 X2=X20
      PRINT 95,X2E(I),X3C,Y3C,Z3C,X3,Y3,Z3
      GO TO 105
  270 Y1=Y10
      PRINT 96,Y1E(I),X3C,Y3C,Z3C,X3,Y3,Z3
      GO TO 105
  280 Y2=Y20
      PRINT 97,Y2E(I),X3C,Y3C,Z3C,X3,Y3,Z3
      GO TO 105
  290 Z1=Z10
      PRINT 98,Z1E(I),X3C,Y3C,Z3C,X3,Y3,Z3
      GO TO 105
  300 Z2=Z20
      PRINT 99,Z2E(I),X3C,Y3C,Z3C,X3,Y3,Z3
      IF(I-8)105,325,325
  325 RETURN
      END
```

Appendix C
Surveyor I Shadow Analysis Data

I. Solution 8

SURVEYOR SHADOW ANALYSIS DATA

GMT				SUN				
DAY	HR	MIN	SEC	EL(THETA)	AZ(PHI)	R	RF	SW
163	10	46	17	26.78	267.10	1.31300	5.00	4.1250

ID	X2	Y2	Z2	X1	Y1	Z1
L3-LK FX	-58.50	34.00	-4.10	13.00	27.40	44.00

L	N	D	V	S	X3	Y3	Z3
86.42	106.34	57.94	15.70	29.685	-57.15	60.46	-17.47

LP	XP	YP	ZP
6.50	18.37	26.90	47.61

ERROR ANALYSIS

VARYING PARAMETER		PERCENTAGE CHANGE IN X3	Y3	Z3	NEW VALUES OF X3	Y3	Z3
THETA	.20 PC	0.000	-.007	.164	-57.159	60.462	-17.503
THETA	-.20 PC	0.000	.007	-.164	-57.158	60.471	-17.446
THETA	.40 PC	0.000	-.015	.328	-57.159	60.457	-17.532
THETA	-.40 PC	0.000	.015	-.328	-57.158	60.476	-17.417
THETA	1.00 PC	.002	-.039	.821	-57.160	60.443	-17.618
THETA	-1.00 PC	-.002	.038	-.820	-57.158	60.490	-17.331
THETA	2.00 PC	.004	-.079	1.644	-57.161	60.418	-17.762
THETA	-2.00 PC	-.004	.076	-1.640	-57.156	60.513	-17.188
PHI	.10 PC	.211	.109	.173	-57.279	60.533	-17.505
PHI	-.10 PC	-.210	-.108	-.171	-57.039	60.401	-17.445
PHI	.20 PC	.423	.218	.349	-57.401	60.599	-17.536
PHI	-.20 PC	-.419	-.217	-.341	-56.919	60.335	-17.415
PHI	.50 PC	1.065	.547	.887	-57.768	60.798	-17.630
PHI	-.50 PC	-1.041	-.542	-.839	-56.564	60.138	-17.328
PHI	2.00 PC	4.420	2.226	3.864	-59.686	61.813	-18.150
PHI	-2.00 PC	-4.032	-2.148	-3.092	-54.854	59.167	-16.934
R	.50 PC	.013	-.249	-.436	-57.166	60.316	-17.398
R	-.50 PC	-.013	.252	.441	-57.151	60.619	-17.552
R	1.00 PC	.026	-.496	-.867	-57.174	60.167	-17.323
R	-1.00 PC	-.027	.507	.887	-57.143	60.774	-17.630
R	2.00 PC	.052	-.980	-1.714	-57.189	59.874	-17.175
R	-2.00 PC	-.055	1.027	1.797	-57.127	61.088	-17.789
R	5.00 PC	.127	-2.370	-4.145	-57.231	59.033	-16.750
R	-5.00 PC	-.142	2.665	4.660	-57.077	62.079	-18.289
SW	.50 PC	-.013	.251	.439	-57.151	60.619	-17.551
SW	-.50 PC	.013	-.250	-.438	-57.166	60.315	-17.398
SW	1.00 PC	-.026	.502	.879	-57.143	60.771	-17.628
SW	-1.00 PC	.026	-.500	-.876	-57.174	60.164	-17.322
SW	2.00 PC	-.053	1.007	1.761	-57.128	61.076	-17.782
SW	-2.00 PC	.053	-1.000	-1.749	-57.189	59.862	-17.169
SW	5.00 PC	-.135	2.531	4.425	-57.081	61.997	-18.248
SW	-5.00 PC	.133	-2.488	-4.350	-57.235	58.962	-16.714
X1	.20 PC	0.000	.007	.013	-57.158	60.471	-17.477
X1	-.20 PC	0.000	-.007	-.013	-57.159	60.462	-17.472
X1	.50 PC	-.001	.019	.033	-57.158	60.478	-17.481
X1	-.50 PC	.001	-.019	-.033	-57.159	60.455	-17.469
X1	1.00 PC	-.002	.038	.067	-57.158	60.490	-17.486
X1	-1.00 PC	.002	-.038	-.067	-57.160	60.443	-17.463
X1	5.00 PC	-.010	.194	.339	-57.153	60.584	-17.534
X1	-5.00 PC	.010	-.193	-.337	-57.165	60.350	-17.416
X2	.20 PC	.202	.034	.060	-57.275	60.488	-17.485
X2	-.20 PC	-.202	-.034	-.060	-57.043	60.446	-17.464
X2	.50 PC	.507	.087	.152	-57.449	60.519	-17.501
X2	-.50 PC	-.507	-.087	-.152	-56.869	60.414	-17.448
X2	1.00 PC	1.014	.174	.305	-57.738	60.572	-17.528
X2	-1.00 PC	-1.014	-.173	-.303	-56.579	60.362	-17.421
X2	5.00 PC	5.070	.881	1.541	-60.057	61.000	-17.744
X2	-5.00 PC	-5.071	-.860	-1.504	-54.260	59.947	-17.212
Y1	.20 PC	0.000	-.017	-.030	-57.159	60.456	-17.469
Y1	-.20 PC	0.000	.017	.031	-57.158	60.477	-17.480
Y1	.50 PC	.002	-.044	-.077	-57.160	60.440	-17.461
Y1	-.50 PC	-.002	.044	.077	-57.157	60.494	-17.488
Y1	1.00 PC	.004	-.088	-.154	-57.161	60.413	-17.448
Y1	-1.00 PC	-.004	.089	.155	-57.156	60.521	-17.502
Y1	5.00 PC	.023	-.430	-.752	-57.172	60.206	-17.343
Y1	-5.00 PC	-.024	.456	.797	-57.145	60.743	-17.614
Y2	.20 PC	-.001	.134	.038	-57.158	60.548	-17.481
Y2	-.20 PC	.001	-.134	-.038	-57.159	60.385	-17.468
Y2	.50 PC	-.002	.336	.096	-57.157	60.670	-17.491
Y2	-.50 PC	.002	-.335	-.095	-57.160	60.264	-17.458
Y2	1.00 PC	-.005	.673	.193	-57.155	60.874	-17.508
Y2	-1.00 PC	.005	-.671	-.190	-57.162	60.061	-17.441
Y2	5.00 PC	-.030	3.381	.997	-57.141	62.511	-17.649
Y2	-5.00 PC	.028	-3.341	-.927	-57.175	58.446	-17.313
Z1	.20 PC	-.001	.031	.055	-57.158	60.486	-17.484
Z1	-.20 PC	.001	-.031	-.055	-57.160	60.448	-17.465
Z1	.50 PC	-.004	.079	.138	-57.156	60.515	-17.499
Z1	-.50 PC	.004	-.078	-.138	-57.161	60.419	-17.450
Z1	1.00 PC	-.008	.158	.277	-57.154	60.563	-17.523
Z1	-1.00 PC	.008	-.157	-.275	-57.164	60.371	-17.426
Z1	5.00 PC	-.042	.800	1.398	-57.134	60.950	-17.719
Z1	-5.00 PC	.041	-.780	-1.364	-57.183	59.995	-17.236
Z2	.20 PC	0.000	.002	.052	-57.159	60.469	-17.484
Z2	-.20 PC	0.000	-.002	-.052	-57.159	60.465	-17.465
Z2	.50 PC	0.000	.007	.130	-57.158	60.471	-17.497
Z2	-.50 PC	0.000	-.007	-.130	-57.159	60.462	-17.452
Z2	1.00 PC	0.000	.014	.260	-57.158	60.476	-17.520
Z2	-1.00 PC	0.000	-.014	-.260	-57.159	60.458	-17.429
Z2	5.00 PC	-.003	.073	1.302	-57.156	60.511	-17.702
Z2	-5.00 PC	.003	-.073	-1.301	-57.161	60.422	-17.247

II. Solution 10A

SURVEYOR SHADOW ANALYSIS DATA

GMT				SUN				
DAY	HR	MIN	SEC	EL(THETA)	AZ(PHI)	R	RF	SW
161	9	29	6	51.80	264.70	1.34400	5.00	1.1560

ID	X2	Y2	Z2	X1	Y1	Z1
P2-GAS JET	60.50	39.60	-9.00	13.00	27.40	44.00

L	N	D	V	S	X3	Y3	Z3
72.20	135.92	39.77	4.30	9.225	61.02	45.28	-16.24

LP	XP	YP	ZP
6.50	8.72	26.30	48.77

ERROR ANALYSIS VARYING PARAMETER		PERCENTAGE CHANGE IN			NEW VALUES OF		
		X3	Y3	Z3	X3	Y3	Z3
THETA	.20 PC	-.001	-.018	.101	61.026	45.272	-16.266
THETA	-.20 PC	.001	.018	-.101	61.027	45.288	-16.233
THETA	.40 PC	-.002	-.036	.203	61.025	45.264	-16.282
THETA	-.40 PC	.002	.035	-.203	61.028	45.297	-16.216
THETA	1.00 PC	-.006	-.091	.506	61.023	45.239	-16.332
THETA	-1.00 PC	.006	.089	-.509	61.030	45.321	-16.167
THETA	2.00 PC	-.012	-.186	1.011	61.019	45.196	-16.414
THETA	-2.00 PC	.012	.175	-1.021	61.034	45.360	-16.083
PHI	.10 PC	-.045	-.034	-.140	60.999	45.265	-16.227
PHI	-.10 PC	.045	.034	.141	61.054	45.296	-16.272
PHI	.20 PC	-.090	-.068	-.278	60.971	45.249	-16.204
PHI	-.20 PC	.092	.068	.284	61.083	45.311	-16.296
PHI	.50 PC	-.225	-.170	-.687	60.889	45.203	-16.138
PHI	-.50 PC	.232	.171	.720	61.168	45.358	-16.367
PHI	2.00 PC	-.862	-.670	-2.566	60.500	44.977	-15.832
PHI	-2.00 PC	.974	.701	3.107	61.621	45.598	-16.754
R	.50 PC	-.004	-.067	-.241	61.024	45.250	-16.210
R	-.50 PC	.004	.068	.244	61.029	45.311	-16.289
R	1.00 PC	-.009	-.135	-.480	61.021	45.219	-16.171
R	-1.00 PC	.009	.138	.490	61.032	45.343	-16.329
R	2.00 PC	-.018	-.267	-.950	61.015	45.159	-16.095
R	-2.00 PC	.019	.279	.992	61.038	45.407	-16.411
R	5.00 PC	-.044	-.647	-2.302	60.999	44.987	-15.875
R	-5.00 PC	.049	.722	2.567	61.057	45.607	-16.667
SW	.50 PC	.004	.068	.242	61.029	45.311	-16.289
SW	-.50 PC	-.004	-.068	-.242	61.024	45.249	-16.210
SW	1.00 PC	.009	.136	.485	61.032	45.342	-16.328
SW	-1.00 PC	-.009	-.136	-.485	61.021	45.218	-16.171
SW	2.00 PC	.018	.273	.972	61.038	45.404	-16.408
SW	-2.00 PC	-.018	-.272	-.969	61.015	45.157	-16.092
SW	5.00 PC	.047	.685	2.438	61.055	45.591	-16.646
SW	-5.00 PC	-.046	-.679	-2.416	60.998	44.973	-15.857
X1	.20 PC	0.000	0.000	.001	61.027	45.280	-16.250
X1	-.20 PC	0.000	0.000	-.001	61.026	45.280	-16.249
X1	.50 PC	0.000	.001	.004	61.027	45.281	-16.250
X1	-.50 PC	0.000	-.001	-.004	61.026	45.280	-16.249
X1	1.00 PC	0.000	.002	.009	61.027	45.281	-16.251
X1	-1.00 PC	0.000	-.002	-.009	61.026	45.279	-16.248
X1	5.00 PC	0.000	.013	.048	61.027	45.286	-16.257
X1	-5.00 PC	0.000	-.012	-.042	61.026	45.275	-16.243
X2	.20 PC	.198	-.002	-.008	61.147	45.279	-16.248
X2	-.20 PC	-.198	.002	.008	60.906	45.281	-16.251
X2	.50 PC	.495	-.005	-.020	61.329	45.278	-16.246
X2	-.50 PC	-.495	.006	.021	60.724	45.283	-16.253
X2	1.00 PC	.990	-.011	-.039	61.631	45.275	-16.243
X2	-1.00 PC	-.990	.012	.045	60.422	45.286	-16.257
X2	5.00 PC	4.953	-.041	-.148	64.050	45.261	-16.225
X2	-5.00 PC	-4.951	.079	.283	58.005	45.316	-16.296
Y1	.20 PC	0.000	-.009	-.034	61.026	45.276	-16.244
Y1	-.20 PC	0.000	.009	.034	61.027	45.285	-16.255
Y1	.50 PC	-.001	-.023	-.085	61.025	45.269	-16.236
Y1	-.50 PC	.001	.024	.085	61.028	45.291	-16.263
Y1	1.00 PC	-.003	-.047	-.170	61.024	45.259	-16.222
Y1	-1.00 PC	.003	.048	.171	61.029	45.302	-16.277
Y1	5.00 PC	-.016	-.235	-.835	61.017	45.174	-16.114
Y1	-5.00 PC	.016	.245	.871	61.037	45.391	-16.391
Y2	.20 PC	0.000	.188	.049	61.027	45.366	-16.257
Y2	-.20 PC	0.000	-.188	-.049	61.026	45.195	-16.241
Y2	.50 PC	.002	.472	.123	61.028	45.494	-16.270
Y2	-.50 PC	-.002	-.471	-.123	61.025	45.067	-16.229
Y2	1.00 PC	.004	.944	.248	61.029	45.708	-16.290
Y2	-1.00 PC	-.004	-.943	-.245	61.024	44.853	-16.210
Y2	5.00 PC	.024	4.730	1.271	61.042	47.422	-16.456
Y2	-5.00 PC	-.023	-4.709	-1.196	61.012	43.148	-16.055
Z1	.20 PC	.001	.017	.060	61.027	45.288	-16.259
Z1	-.20 PC	-.001	-.017	-.060	61.026	45.273	-16.240
Z1	.50 PC	.002	.042	.152	61.028	45.300	-16.274
Z1	-.50 PC	-.002	-.042	-.152	61.025	45.261	-16.225
Z1	1.00 PC	.005	.085	.304	61.030	45.319	-16.299
Z1	-1.00 PC	-.005	-.085	-.304	61.023	45.242	-16.200
Z1	5.00 PC	.029	.430	1.532	61.045	45.475	-16.498
Z1	-5.00 PC	-.029	-.424	-1.511	61.009	45.088	-16.004
Z2	.20 PC	0.000	.003	.123	61.027	45.282	-16.269
Z2	-.20 PC	0.000	-.003	-.123	61.026	45.279	-16.229
Z2	.50 PC	0.000	.008	.308	61.027	45.284	-16.300
Z2	-.50 PC	0.000	-.008	-.308	61.026	45.276	-16.199
Z2	1.00 PC	.001	.017	.616	61.027	45.288	-16.350
Z2	-1.00 PC	-.001	-.017	-.616	61.026	45.272	-16.149
Z2	5.00 PC	.006	.087	3.081	61.030	45.320	-16.750
Z2	-5.00 PC	-.006	-.087	-3.080	61.023	45.241	-15.749

III. Solution 15

SURVEYOR SHADOW ANALYSIS DATA

GMT DAY	HR	MIN	SEC	SUN EL(THETA)	AZ(PHI)	R	RF	SW
153	7	43	9	29.40	91.20	.96900	5.00	.8440

ID	X2	Y2	Z2	X1	Y1	Z1
P2-TOP C3	69.20	33.00	-13.60	13.00	27.40	44.00

L	N	D	V	S	X3	Y3	Z3
80.66	107.62	68.02	4.35	7.138	69.33	26.78	-17.10

LP	XP	YP	ZP
6.50	8.47	26.94	48.64

ERROR ANALYSIS

VARYING PARAMETER		PERCENTAGE CHANGE IN X3	Y3	Z3	NEW VALUES OF X3	Y3	Z3
THETA	.20 PC	0.000	.006	.043	69.330	26.784	-17.111
THETA	-.20 PC	0.000	-.006	-.043	69.330	26.780	-17.096
THETA	.40 PC	0.000	.013	.086	69.330	26.786	-17.118
THETA	-.40 PC	0.000	-.013	-.086	69.330	26.778	-17.089
THETA	1.00 PC	0.000	.034	.215	69.330	26.791	-17.140
THETA	-1.00 PC	0.000	-.034	-.215	69.330	26.773	-17.067
THETA	2.00 PC	0.000	.069	.431	69.329	26.801	-17.177
THETA	-2.00 PC	0.000	-.067	-.430	69.330	26.764	-17.030
PHI	.10 PC	.014	-.008	.008	69.340	26.780	-17.105
PHI	-.10 PC	-.014	.008	-.008	69.320	26.784	-17.102
PHI	.20 PC	.028	-.017	.016	69.350	26.777	-17.106
PHI	-.20 PC	-.028	.017	-.016	69.310	26.787	-17.101
PHI	.50 PC	.071	-.043	.042	69.380	26.770	-17.111
PHI	-.50 PC	-.071	.043	-.041	69.280	26.794	-17.096
PHI	2.00 PC	.289	-.170	.174	69.530	26.737	-17.133
PHI	-2.00 PC	-.284	.179	-.161	69.132	26.830	-17.076
R	.50 PC	0.000	.118	-.104	69.329	26.814	-17.086
R	-.50 PC	0.000	-.120	.105	69.330	26.750	-17.122
R	1.00 PC	-.001	.236	-.208	69.328	26.845	-17.068
R	-1.00 PC	.001	-.241	.212	69.331	26.717	-17.140
R	2.00 PC	-.003	.467	-.413	69.327	26.907	-17.033
R	-2.00 PC	.003	-.487	.430	69.332	26.651	-17.177
R	5.00 PC	-.009	1.135	-1.002	69.323	27.086	-16.932
R	-5.00 PC	.010	-1.258	1.111	69.337	26.445	-17.294
SW	.50 PC	0.000	-.119	.105	69.330	26.750	-17.122
SW	-.50 PC	0.000	.119	-.105	69.329	26.814	-17.086
SW	1.00 PC	.001	-.238	.210	69.331	26.718	-17.140
SW	-1.00 PC	-.001	.238	-.210	69.328	26.846	-17.068
SW	2.00 PC	.003	-.477	.421	69.332	26.654	-17.176
SW	-2.00 PC	-.003	.477	-.421	69.327	26.910	-17.032
SW	5.00 PC	.009	-1.195	1.055	69.336	26.462	-17.284
SW	-5.00 PC	-.009	1.192	-1.052	69.323	27.101	-16.924
X1	.20 PC	0.000	.004	-.003	69.330	26.783	-17.103
X1	-.20 PC	0.000	-.004	.003	69.330	26.781	-17.104
X1	.50 PC	0.000	.010	-.009	69.330	26.785	-17.102
X1	-.50 PC	0.000	-.010	.009	69.330	26.779	-17.105
X1	1.00 PC	0.000	.021	-.018	69.330	26.788	-17.100
X1	-1.00 PC	0.000	-.021	.018	69.330	26.776	-17.107
X1	5.00 PC	0.000	.104	-.092	69.329	26.810	-17.088
X1	-5.00 PC	0.000	-.105	.093	69.330	26.754	-17.120
X2	.20 PC	.199	-.022	.019	69.468	26.776	-17.107
X2	-.20 PC	-.199	.022	-.019	69.191	26.788	-17.100
X2	.50 PC	.499	-.056	.049	69.676	26.767	-17.112
X2	-.50 PC	-.499	.055	-.049	68.983	26.797	-17.095
X2	1.00 PC	.999	-.112	.099	70.022	26.752	-17.121
X2	-1.00 PC	-.999	.111	-.098	68.637	26.812	-17.087
X2	5.00 PC	4.995	-.570	.503	72.793	26.629	-17.190
X2	-5.00 PC	-4.995	.550	-.485	65.867	26.929	-17.021
Y1	.20 PC	0.000	-.004	.004	69.330	26.781	-17.104
Y1	-.20 PC	0.000	.004	-.004	69.330	26.783	-17.103
Y1	.50 PC	0.000	-.012	.010	69.330	26.779	-17.105
Y1	-.50 PC	0.000	.012	-.010	69.330	26.785	-17.102
Y1	1.00 PC	0.000	-.025	.022	69.330	26.775	-17.107
Y1	-1.00 PC	0.000	.024	-.021	69.330	26.789	-17.100
Y1	5.00 PC	.001	-.130	.115	69.330	26.747	-17.123
Y1	-5.00 PC	0.000	.116	-.103	69.329	26.813	-17.086
Y2	.20 PC	0.000	.252	-.005	69.330	26.850	-17.103
Y2	-.20 PC	0.000	-.252	.005	69.330	26.714	-17.105
Y2	.50 PC	0.000	.630	-.013	69.330	26.951	-17.101
Y2	-.50 PC	0.000	-.631	.013	69.330	26.613	-17.106
Y2	1.00 PC	0.000	1.261	-.025	69.330	27.120	-17.099
Y2	-1.00 PC	0.000	-1.262	.026	69.330	26.444	-17.108
Y2	5.00 PC	-.001	6.299	-.122	69.329	28.469	-17.083
Y2	-5.00 PC	.001	-6.319	.140	69.331	25.089	-17.128
Z1	.20 PC	0.000	-.019	.017	69.330	26.777	-17.107
Z1	-.20 PC	0.000	.019	-.017	69.330	26.787	-17.101
Z1	.50 PC	0.000	-.049	.043	69.330	26.769	-17.111
Z1	-.50 PC	0.000	.049	-.043	69.329	26.795	-17.096
Z1	1.00 PC	0.000	-.098	.086	69.330	26.756	-17.118
Z1	-1.00 PC	0.000	.098	-.086	69.329	26.808	-17.089
Z1	5.00 PC	.004	-.496	.437	69.333	26.649	-17.179
Z1	-5.00 PC	-.003	.487	-.430	69.327	26.913	-17.030
Z2	.20 PC	0.000	-.006	.164	69.330	26.780	-17.132
Z2	-.20 PC	0.000	.006	-.164	69.330	26.784	-17.075
Z2	.50 PC	0.000	-.015	.410	69.330	26.778	-17.174
Z2	-.50 PC	0.000	.015	-.410	69.330	26.786	-17.033
Z2	1.00 PC	0.000	-.030	.821	69.330	26.774	-17.244
Z2	-1.00 PC	0.000	.030	-.821	69.330	26.790	-16.963
Z2	5.00 PC	.001	-.152	4.110	69.331	26.741	-17.807
Z2	-5.00 PC	-.001	.151	-4.109	69.329	26.823	-16.401